Journal of Statistical Mechanics: Theory and Experiment
An IOP and SISSA journal

Potential energy landscape description of supercooled liquids and glasses

Francesco Sciortino

Dipartimento di Fisica, INFM UdR and CRS Soft: Complex Dynamics in Structured Systems, Università di Roma La Sapienza, Piazzale Aldo Moro 2, 00185 Roma, Italy
E-mail: francesco.sciortino@phys.uniroma1.it

Received 21 April 2005
Accepted 4 May 2005
Published 31 May 2005

Online at stacks.iop.org/JSTAT/2005/P05015
doi:10.1088/1742-5468/2005/05/P05015

Abstract. These notes review the potential energy landscape thermodynamic formalism and some of its recent applications to the study of supercooled glass forming liquids. They also review the techniques which have been recently developed to quantify the statistical properties of the landscape, i.e. the number and the distribution in energy of the local minima of the surface for bulk systems. A critical examination of the approximations involved in such a calculation and results for models of simple and molecular liquids are reported. Finally, these notes discuss how an equation of state, expressed only in terms of statistical properties of the landscape, can be derived and under which conditions such an equation of state can be generalized to describe out-of-equilibrium liquids.

Keywords: energy landscapes (theory), memory effects (theory), slow dynamics and ageing (theory), supercooled liquids (theory)

J. Stat. Mech. (2005) P05015

Contents

1. Introduction

The most fascinating phenomenon taking place in supercooled glass forming liquids [1]–[4]—i.e. liquids where a metastable equilibrium is reached in a time shorter than the crystallization time[1]—is the slowing down of the dynamics. On cooling, the characteristic

[1] In 'metastable equilibrium' supercooled states, no drift of the one-time quantities (energy, pressure, and so on) is observed and correlation functions depend only on time differences. Still, from a thermodynamic point of view the liquid has a free energy higher than the crystal one. On timescales much longer than the characteristic structural time of the liquid, a transition to a crystal state will take place.

J. Stat. Mech. (2005) P05015

times increase by more than 15 orders of magnitude in a relatively small temperature interval. According to the T dependence of the characteristic relaxation time (or of the viscosity), two extreme classes of liquids can be defined [5]: *strong* liquids, mostly network forming, for which an Arrhenius dependence describes the slowing down of the dynamics well (suggesting a divergence of the characteristic time only at $T = 0$ K) and *fragile* liquids, where a super-Arrhenius dependence is observed, suggesting a possible divergence of the characteristic time at a finite T. The glass transition temperature T_g is conventionally defined as the T at which the characteristic time becomes of the order of 100 s. For T lower than T_g metastable equilibrium is hardly reached within the experimental time window and one-time quantities evolve with time t. Similarly, correlation functions depend not only on time differences but also on the previous sample history.

The slowing down of the dynamics preceding the glass transition is accompanied by another interesting phenomenon [6]: a significant decrease of the excess entropy ΔS_{ex}, defined as the entropy of the liquid minus the entropy of the crystal. ΔS_{ex} indicates (with some caveats) the number of distinct microscopic configurations available to the liquid as compared to the 'unique' crystalline configuration[2]. The fast decrease of ΔS_{ex} suggests a progressive reduction of the number of configurations explored on supercooling. In the case of fragile liquids, the apparent divergence of the characteristic times is mirrored by the apparent vanishing of the excess entropy, indicating a correlation between thermodynamic and dynamic properties. The divergence of the characteristic times and the vanishing of ΔS_{ex} are located below T_g and hence are not experimentally accessible. Strong and fragile liquids can also be discriminated according to their thermodynamic properties [7]. Fragile liquids tend to exhibit large changes in the specific heat around T_g as compared to strong ones.

Another important property of the dynamics of supercooled liquids is the development of a separation of timescales. The short microscopic dynamics is not much affected by supercooling, while the structural relaxation time (the so-called α relaxation, describing the long time decay of correlation functions) is significantly changed by T (according to the fragile/strong character of the system). This separation of timescales appears very clearly in the shape of the correlation functions, when plotted on a $\log t$ scale to cover both short and long times. The decay of the correlation is characterized by a fast relaxation toward a plateau, followed by the much slower α relaxation to zero. Goldstein [8] interpreted this separation of timescales, suggesting that molecular motions in supercooled liquids consist of anharmonic vibrations about deep potential energy minima and of infrequent visitations of different such minima, stimulating the interest in a study of the properties of the potential energy landscape (PEL) sampled in supercooled states.

The ultimate goal of any theory for supercooled liquids is understanding the slowing down of the dynamics and the differences between strong and fragile behaviour[3], starting from the microscopic interparticle potential. Despite this, in these notes I will focus

[2] To grasp the meaning of ΔS_{ex}, let us suppose that the liquid and the crystal have the same vibrational properties (the same vibrational density of states). In this case, the vibrational entropy (i.e. the region of configuration space explored during the vibrational motion) of the liquid and of the crystal would be the same and the excess entropy would only count the number of distinct microscopic configurations available to the liquid as compared to the unique crystalline configuration.

[3] For a recent review of the connection between PEL and strong–fragile behaviour see [9].

only on the thermodynamic side of the PEL approach. In particular I will discuss recent developments in the study of the statistical properties of the PEL, triggered by the enhancement of computer power available. I will show how the knowledge of the PEL sampled in equilibrium provides important information on the thermodynamics of glasses, when glasses can be approximated as frozen liquid configurations. In the near future, emphasis will have to switch more and more from thermodynamics to dynamics[4] with the hope that the central dogma of supercooled liquids[5]—i.e. the hypothesis that dynamics is slaved to statics—will provide a stable foundation for understanding of slow dynamics in glass forming liquids within the PEL approach.

2. The PEL

What is the PEL, or equivalently the potential energy surface (PES)[6]? It is a fancy word for the potential energy $V(\vec{r}^N)$ of a system of N particles (which for simplicity here we assume to be point-like) as a function of the $3N$ coordinates $\vec{r}^N$.[7] At any instant of time, the system is described by a specific $\vec{r}^N$ value. Pictorially, the trajectory of the system can be represented as a motion of a representative point on the $V(\vec{r}^N)$ surface. It is important to stress that the PEL does not depend on T. It is also important to realize that the exploration of the PEL (i.e. which parts of the surface are explored) is strongly T dependent. As the surface is in $3N$-dimensional space, the characterization of the surface can only be performed on a statistical basis, and one of the aims of the PEL studies is indeed to estimate the number of local minima and their distribution in energy, and to estimate the shape of the surface around the local minimum and the hypervolume in configuration space associated with each of these minima. The number and energy depth of the local minima are indeed the basic ingredients of the PEL thermodynamic formalism, put on a firm basis by the work of Stillinger and Weber [12]. Stillinger and Weber provided a formally exact partitioning of the configurational space as a sum of distinct basins, associating with each local minimum of the potential energy surface (named an inherent structure, IS) all points in configuration space connected to the minimum by a steepest descent path. This set of points is named a *basin*. The definition of a basin proposed by Stillinger and Weber provides the essential ingredient for developing a thermodynamic formalism since—except for a set of points of zero measure (the saddles and the ridges between different basins)—all points in configuration space are associated with a local minimum. The Stillinger and Weber definition also provides an algorithm suited for numerical studies of the landscape properties.

[4] Connections between PEL properties and dynamics in liquids already have a long history. Research has proceeded along several parallel directions: instantaneous normal mode (INM), Adam–Gibbs (AG), inherent saddle and barrier approaches. One reference connecting PEL properties to dynamics is [10].

[5] Harrowell, in his talk at the UCGPC, Bangalore 2004, proposed naming the hypothesis that dynamics is slaved to statics (or thermodynamics) as 'the central dogma'. Of course, this idea lies behind most of the theories of the glass transition (including MCT).

[6] For a very good introduction to the concept of the energy landscape, see [11].

[7] Ideas introducing the concept of the energy landscape and its use in statistical mechanics can be traced to the early work of people like Briant, Burton, Etters and McGinty, to name but a few. In these notes, I will mostly focus on the Stillinger and Weber formalization of these ideas [12] to bulk liquids. It is important to stress that extremely relevant thermodynamic developments of the PEL ideas, not discussed here, have taken place in the study of isolated clusters. The interested reader is referred to [11] for further details.

doi:10.1088/1742-5468/2005/05/P05015

3. Stillinger–Weber thermodynamics formalism

In this section I will review the PEL thermodynamic formalism. The partition function Z of a system of N particles interacting via a two-body spherical potential is[8]

$$Z(T,V) = \frac{1}{N!\lambda^{3N}} Q(V,T) \tag{1}$$

with

$$Q(V,T) = \int_V \mathrm{e}^{-\beta V(\vec{r}^N)}\, \mathrm{d}\vec{r}^N, \tag{2}$$

where λ is the de Broglie wavelength, $\beta = 1/k_\mathrm{B}T$ and k_B is the Boltzmann constant.

The idea that the configuration space can be partitioned into basins allows us to write the partition function as a sum over the partition functions of the individual distinct basins Q_i:

$$Q(T,V) = {\sum_i}' Q_i(T,V). \tag{3}$$

To model the thermodynamics of the supercooled state the sum has to exclude (and the sign $'$ in $\sum$ has this role) all basins which include a significant fraction of crystalline order[9]. Indicating by e_IS the value of the energy in the local minimum and with $\Delta V(\vec{r}^N) \equiv V(\vec{r}^N) - e_\mathrm{IS}$,

$$Q_i(T,V) = \mathrm{e}^{-\beta e_{\mathrm{IS}_i}} \int_{\text{basin } i} \mathrm{e}^{-\beta \Delta V(\vec{r}^N)}\, \mathrm{d}\vec{r}^N. \tag{4}$$

Next we define a partition function averaged over all distinct basins with the same e_IS value as

$$Q(e_\mathrm{IS},T,V) = \frac{\sum_i \delta_{e_{\mathrm{IS}_i},e_\mathrm{IS}} Q_i(T,V)}{\sum_i \delta_{e_{\mathrm{IS}_i},e_\mathrm{IS}}} \tag{5}$$

and the associated average basin free energy as

$$-\beta f_\mathrm{basin}(e_\mathrm{IS},T,V) \equiv \ln\left[\frac{Q(e_\mathrm{IS},T,V)}{\lambda^{3N}}\right]. \tag{6}$$

The system partition function can be written as

$$Z(T,V) = \sum_{e_\mathrm{IS}} \Omega(e_\mathrm{IS}) \mathrm{e}^{-\beta f_\mathrm{basin}(e_\mathrm{IS},T,V)} \tag{7}$$

where $\Omega(e_\mathrm{IS}) = \sum_i \delta_{e_{\mathrm{IS}_i},e_\mathrm{IS}}$ counts the number of basins of depth e_IS. Note that the $N!$ term disappears since the sum is now over all distinct basins (i.e. an IS is invariant for permutation of identical particles).

[8] Symmetry is ignored in the discussion in section 3 since these notes are focused on disordered liquid configurations, for which all the structures lack any point group symmetry elements (aside from the identity). In the case of clusters and finite systems, the equations in section 3 need to be modified to account for the system symmetries. Neglecting symmetries may lead to significantly erroneous free energy estimates. See [11] for a comprehensive discussion of the role of symmetries in PEL studies of clusters.

[9] The amount of crystalline order can be quantified by calculating appropriate rotational invariants or by analysing the value of the density fluctuations at all the wavevectors close to the first peak of the structure factor.

J. Stat. Mech. (2005) P05015

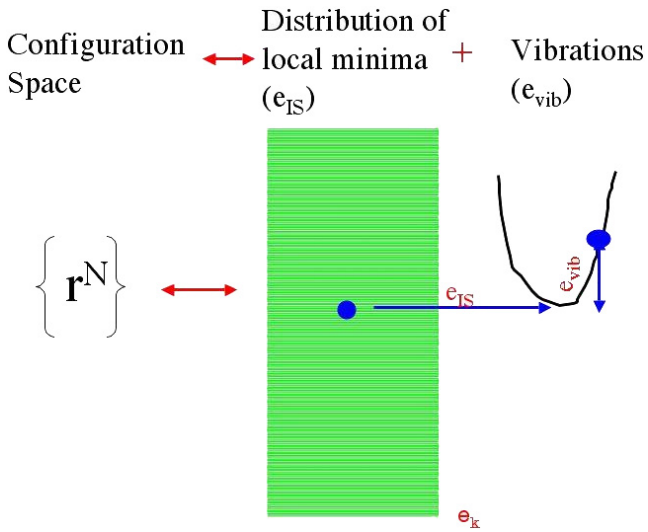

Figure 1. Schematic representation of a system in the PEL framework. The energy levels indicate the possible values of $e_{\rm IS}$, bounded from below by $e_{\rm K}$, defined as the lowest IS energy of a non-crystalline configuration. Each IS is associated with a different basin. The potential energy of the system $V(\vec{r}^N)$ is expressed as sum of $e_{\rm IS}$ and a vibrational component $e_{\rm vib} \equiv V(\vec{r}^N) - e_{\rm IS}$.

Defining the configurational entropy $S_{\rm conf}(e_{\rm IS})$ as

$$S_{\rm conf}(e_{\rm IS}) \equiv k_{\rm B} \ln[\Omega(e_{\rm IS})] \tag{8}$$

a formally exact expression for $Z(T,V)$ can be written as

$$Z(T,V) = \sum_{e_{\rm IS}} {\rm e}^{-\beta[-TS_{\rm conf}(e_{\rm IS}) + f_{\rm basin}(e_{\rm IS},T,V)]}. \tag{9}$$

All quantities appearing in the argument of the exponential scale linearly with the number of particles N. In the thermodynamic limit, only the value of $e_{\rm IS}$ which maximizes the argument will contribute to the sum. In this saddle point approximation $Z(T,V)$ can be written as

$$Z(T,V) = {\rm e}^{-\beta[-TS_{\rm conf}(\langle e_{\rm IS}\rangle) + f_{\rm basin}(\langle e_{\rm IS}\rangle,T,V)]}, \tag{10}$$

where $\langle e_{\rm IS}\rangle$, a function of T and V, is the solution of

$$T\frac{\partial S_{\rm conf}(e_{\rm IS})}{\partial e_{\rm IS}}\bigg|_V - \frac{\partial f_{\rm basin}(e_{\rm IS},T,V)}{\partial e_{\rm IS}}\bigg|_V = 1. \tag{11}$$

The resulting free energy can be written as

$$F(T,V) = -TS_{\rm conf}(\langle e_{\rm IS}\rangle) + f_{\rm basin}(\langle e_{\rm IS}\rangle,T,V). \tag{12}$$

This expression for F reflects the fact that the free energy of the liquid can be written as the free energy of the liquid *constrained* to being in one of its characteristic basins (the term $f_{\rm basin}(\langle e_{\rm IS}\rangle,T,V)$) plus an entropic term $(-TS_{\rm conf}(\langle e_{\rm IS}\rangle))$ which counts the number of basins explored at temperature T. As described in figure 1, the state of the system, which is usually represented as a point $\vec{r}^N$, is in the IS formalism represented as a point

in a collection of energy levels, and each level labels one of the distinct PEL basins. With each level there is associated a basin shape, which, according to T, weights in a different way the basin probability.

In these notes I have chosen to work in the canonical ensemble, evaluating the V and T dependence of the thermodynamic potential. In this case, the PEL is defined by the coordinates of the system. On changing V, the PEL changes [11, 13]. Local minima result from steepest descent minimization of the energy at constant V. An alternative but thermodynamically equivalent formalism can be derived for the P–T ensemble, where enthalpy replaces energy. The enthalpy landscape (which now depends on P) requires simultaneous minimization of the coordinates and volume. Although it is not commonly studied numerically [14, 15], the enthalpy landscape has a direct link to experimental studies [16]–[18]. Also, the minimization procedure, being carried out at constant P, does not interfere with liquid–gas phase separation phenomena [19], as is the case for constant volume minimizations at low densities [20].

3.1. A simple example

As an example of the previous derivation, we calculate the partition function Q for a one-dimensional landscape, defined by the function $V(x) = V_o \cos[(2\pi n/L)x]$, defined between 0 and L. The landscape for this model is composed of n basins, each with $e_{IS} = -1$ and 'size' L/n. The Stillinger–Weber procedure would give

$$Q = \int_0^L \mathrm{e}^{-\beta V(x)}\,\mathrm{d}x = \sum_{i=0}^{n-1} Q_i \tag{13}$$

with

$$Q_i = \int_{i(L/n)}^{(i+1)(L/n)} \mathrm{e}^{-\beta V(x)}\,\mathrm{d}x. \tag{14}$$

Since all basins have the same depth, $Q = nQ_0$, and F can be written as a sum of an entropic and a free energy term as $F = -T\ln[n] + f_{\mathrm{basin}}$, with $-\beta f_{\mathrm{basin}} = \ln[Q_0]$.

4. Simulation details

A proper analysis of equilibrium configurations, generated via molecular dynamics or Monte Carlo techniques, if interpreted using the thermodynamic formalism discussed before, allows us to extract information on the statistical properties of the landscape (i.e. on the function $\Omega(e_{IS})$ and on the relation between the basin depth e_{IS} and the basin shape). Indeed $F(T, V)$ (the left side in equation (12)) can be calculated numerically, with arbitrary precision, via standard thermodynamic integration techniques [21]–[25], along a path which starts from the ideal gas (for which an exact expression for the free energy is known) reaching the final (T, V) liquid state point. The path can be chosen in an arbitrary way, but must avoid any intersection with the liquid–gas coexistence curve. The basin free energy, as discussed below, can also be evaluated numerically. The difference between $F(T, V)$ and $f_{\mathrm{basin}}(T, V)$ provides an estimate of the number of basins with energy $\langle e_{IS}\rangle$.

The IS configurations explored at temperature T can be numerically evaluated by a steepest descent minimization of the potential energy starting from equilibrium

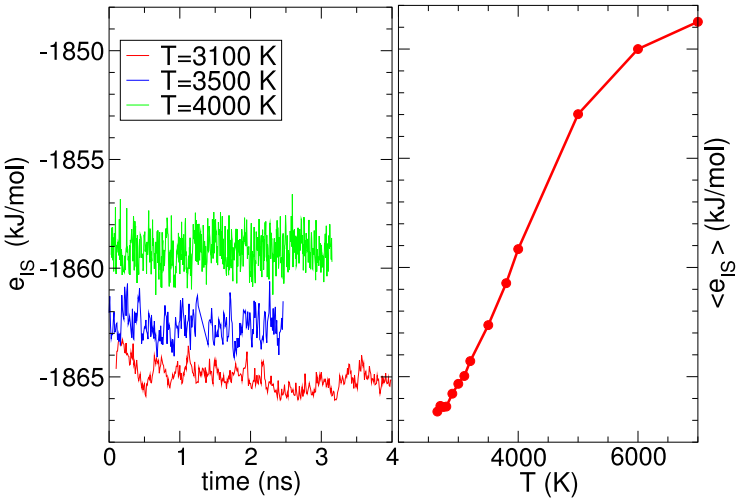

Figure 2. Left: time dependence of $e_{\rm IS}$ for the BKS model for silica in a 999-ion system for three different temperatures. Note that at each T, a different set of $e_{\rm IS}$ values is sampled. Right: T dependence of $\langle e_{\rm IS}\rangle$ for the same model.

configurations. To improve numerical efficiency, the slow steepest descent algorithm is often replaced by the conjugate-gradient algorithm. The code provided by *Numerical Recipes* [26] can be quickly adapted to the case of atomic liquids. A reasonable estimate of $\langle e_{\rm IS}\rangle$ for a 1000-atom system is reached with about 50 minimizations of independent configurations. If the distribution of $e_{\rm IS}$ sampled at temperature T, $P(e_{\rm IS}, T)$ [23] must be evaluated, about 1000 configurations should be minimized.

In these notes I will show data for different model potentials, encompassing atomic and molecular systems. Most of the data will be based on the well characterized 80–20 Lennard-Jones binary mixture developed by Stillinger [27] and optimized by Kob and Andersen [28][10]. I will also show data for a 50–50 soft sphere (SS) binary mixture [22], in which particles interact with a self-similar repulsive r^{-12} potential.

I will present data for the BKS model for silica [29], as a model of a strong atomic liquid, where O and Si are explicitly modelled as ions. For rigid molecular systems I will show data for a simple model for ortho-terphenyl, proposed by Lewis and Wahnström [30], and for the SPC/E model of water [31]. The OTP model is essentially a LJ-type potential, while the SPC/E model includes electrostatic and LJ interactions.

5. $e_{\rm IS}$

Figure 2 shows the time evolution of $e_{\rm IS}$ following a MD trajectory (left panel) and the T dependence of $\langle e_{\rm IS}\rangle$ (right panel) for BKS silica. It is interesting to observe that there is a characteristic depth sampled at each temperature. For a 1000-atom system, fluctuations in $e_{\rm IS}$ are already small and it is extremely rare to sample basins of depth much different from $\langle e_{\rm IS}\rangle$. This clearly shows that the probability of locating deep energy basins starting from configurations equilibrated at high T is extremely low. The low

[10] Note that there are different versions of the BMLJ model in current use, differing in the cut-off and tapering of the potential.

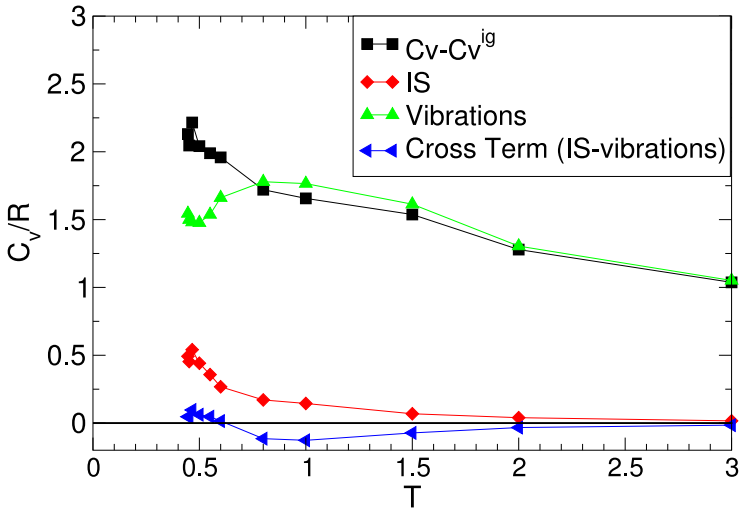

Figure 3. Energy fluctuations, divided by $Nk_{\rm B}T^2$, for the BMLJ system. The total and its three contributions are shown. Here T is measured in units of the LJ depth. When $T < T_{\rm o} \approx 1$, correlation functions start to show stretched exponential decays and the T dependence of the $\langle e_{\rm IS}\rangle$ starts to drop. Note that the low T increase in C_v arises from the fluctuations in $e_{\rm IS}$, while the vibrational component approaches the classical $(3/2)k_{\rm B}$ harmonic limit.

energy basins are not sampled, even if an extremely large number of high T equilibrium configurations are minimized. Only for system size smaller than 50 atoms do fluctuations in $e_{\rm IS}$ become comparable to the range of possible $e_{\rm IS}$ values and can all possible basins be accessed with small but finite probability even starting from high T (even random) configurations [32, 33]. For systems of size 100 particles or more, low energy basins are found [34] only if the equilibrium configurations are representative of supercooled states. Sastry *et al* [34] made the very important observation that the T at which the system starts to explore low energy basins (sometimes named the onset temperature, $T_{\rm o}$) coincides with the onset of stretched exponential decay in the correlation functions. Reference [34] suggested that at $T_{\rm o}$ microscopic and structural relaxation times start to separate and the ideas behind the PEL approach acquire progressive relevance.

At the basis of the PEL approach (see figure 1) lies the separation of the potential energy into $e_{\rm IS}$ and the vibrational component $e_{\rm vib}$. This separation helps us to understand the origin of the increase in specific heat observed in supercooled states. Indeed, the excess (over the ideal gas) specific heat $C_V^{\rm ex}$ can be written in terms of fluctuations of the potential energy E as

$$C_V = \frac{\langle \Delta E^2\rangle}{k_{\rm B}T^2}. \tag{15}$$

In the PEL approach, since $E = e_{\rm IS} + e_{\rm vib}$,

$$\langle \Delta E^2\rangle = \langle \Delta e_{\rm IS}^2\rangle + \langle \Delta e_{\rm vib}^2\rangle + \langle \Delta e_{\rm IS}\Delta e_{\rm vib}\rangle. \tag{16}$$

Figure 3 shows the three contributions to the specific heat for the BMLJ case. Below the onset temperature ($T_{\rm o} \approx 1$ for BMLJ) the significant increase in the specific heat

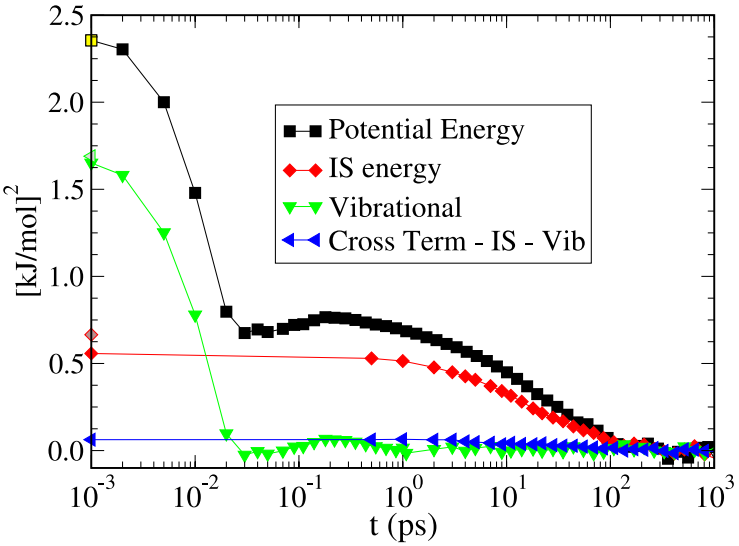

Figure 4. Autocorrelation function of the potential energy fluctuations decomposed into $e_{\rm IS}$ and $e_{\rm vib}$ components. Data refer to BKS silica at $T = 3500$ K and $\rho = 2.36$ g cm^{-3}.

arises from the fluctuations in the basin depth, while the vibrational component appears to saturate to the harmonic limit. A small cross-term is also present, attesting to a weak coupling between the vibrational and configurational properties.

It is also instructive to study the time dependent autocorrelation function of the energy fluctuations. This quantity provides information on the time dependent specific heat (or, in frequency space, on its frequency dependence [35]). As before, $\langle \Delta E(t) \Delta E(0) \rangle$ can be separated as

$$\langle \Delta E(t) \Delta E(0) \rangle = \langle \Delta e_{\rm IS}(t) \Delta e_{\rm IS}(0) \rangle + \langle \Delta e_{\rm vib}(t) \Delta e_{\rm vib}(0) \rangle + 2 \langle \Delta e_{\rm IS}(t) \Delta e_{\rm vib}(0) \rangle. \quad (17)$$

Figure 4 shows these three autocorrelation functions for the case of BKS silica. The short time (high frequency) contributions to C_V are originated by the vibrational properties, and decay to zero on a microscopic timescale. The long time α relaxation dynamics is mostly ascribed to the $e_{\rm IS}$ autocorrelation function. A small, but not negligible, slow contribution—evidence of basin dependent anharmonic effects—is provided by the cross-term.

6. The basin free energy

6.1. The harmonic approximation

The potential energy around an IS configuration can be expanded in a quadratic form:

$$V(\vec{r}^N) \approx e_{\rm IS} + \sum_{i,j,\alpha,\beta} H_{i\alpha j\beta} \delta r_i^\alpha \delta r_j^\beta \quad (18)$$

where the Hessian matrix H has components

$$H_{i\alpha j\beta} = \left. \frac{\partial^2 V(\vec{r}^N)}{\partial r_i^\alpha \partial r_j^\beta} \right|_{\rm IS} \quad (19)$$

and δr_i^α indicates the displacement from the IS configuration of atom i in direction α. Diagonalization of the mass weighted Hessian matrix (with elements $(1/\sqrt{m_i m_j})H_{i\alpha j\beta}$) provides a set of $3N$ independent directions (eigenvectors) and $3N$ curvatures (eigenvalues ω^2). In the basis of the eigenvectors, the dynamics of the system can be described as a sum of $3N$ independent oscillations with frequencies ω_i. In the harmonic approximation, the partition function of a single basin i can thus be expressed as

$$Z(e_{\mathrm{IS}_i}, T, V) = \mathrm{e}^{-\beta e_{\mathrm{IS}_i}} \prod_{j=1}^{3N} [\beta\hbar\omega_j(e_{\mathrm{IS}_i})]^{-1}. \tag{20}$$

The partition function averaged over all basins with the same depth e_{IS} (equation (5)) becomes

$$Z(e_{\mathrm{IS}}, T, V) = \mathrm{e}^{-\beta e_{\mathrm{IS}}} \left\langle \prod_{j=1}^{3N} [\beta\hbar\omega_j(e_{\mathrm{IS}})]^{-1} \right\rangle_{e_{\mathrm{IS}}} \tag{21}$$

which, by going from the product to the exponential of the sum, can be written as

$$Z(e_{\mathrm{IS}}, T, V) = \mathrm{e}^{-\beta e_{\mathrm{IS}}} \langle \mathrm{e}^{-\sum_{j=1}^{3N} \ln[\beta\hbar\omega_j(e_{\mathrm{IS}})]} \rangle_{e_{\mathrm{IS}}}. \tag{22}$$

The corresponding resulting expression for the basin free energy in the harmonic approximation is

$$\begin{aligned} -\beta f_{\mathrm{basin}}(e_{\mathrm{IS}}, T, V) &= -\beta e_{\mathrm{IS}} - \beta f_{\mathrm{vib}}(e_{\mathrm{IS}}, T, V) \\ -\beta f_{\mathrm{vib}}(e_{\mathrm{IS}}, T, V) &\equiv \ln[\langle \mathrm{e}^{-\sum_{j=1}^{3N} \ln[\beta\hbar\omega_j(e_{\mathrm{IS}})]} \rangle_{e_{\mathrm{IS}}}]. \end{aligned} \tag{23}$$

In many PEL studies, f_{vib} has been approximated as

$$\beta f_{\mathrm{vib}}(e_{\mathrm{IS}}, T, V) = -\left\langle \sum_{j=1}^{3N} \ln[\beta\hbar\omega_j(e_{\mathrm{IS}})] \right\rangle_{e_{\mathrm{IS}}}. \tag{24}$$

It is worth noting that an appropriate evaluation of f_{vib} requires an average over independent basins with the same depth. Numerically it is often performed over the IS generated minimizing equilibrium configurations, which are of course sampled according to their statistical Boltzmann weight.

In the harmonic approximation, the basin free energy can be written as a sum of a term which is only T dependent and a term which accounts for the shape of the basin. The shape contribution $\mathcal{S}$, defined as

$$\mathcal{S}(e_{\mathrm{IS}}) \equiv \left\langle \sum_{j=1}^{3N} \ln[\omega_j(e_{\mathrm{IS}})/\omega_0] \right\rangle_{e_{\mathrm{IS}}} \tag{25}$$

where ω_0 is the unit frequency making the argument of the ln adimensional, encodes the possible coupling between depth and shape at harmonic level. It has been found numerically that $\mathcal{S}$ has a linear [36], [25, 37, 38] or weakly quadratic [11, 23, 39] dependence on e_{IS}. In terms of $\mathcal{S}$, the harmonic vibrational free energy can be written as (see the approximation in equation (24))

$$f_{\mathrm{vib}}(e_{\mathrm{IS}}, T, V) = -3NkT \ln[\beta\hbar\omega_0] - kT\mathcal{S}(e_{\mathrm{IS}}). \tag{26}$$

J. Stat. Mech. (2005) P05015

The harmonic approximation captures a significant part of the relation between the shape and depth. Still, it remains an approximation which needs to be improved. An indication of the necessity for improving on the harmonic approximation is encoded in the non-zero value of the cross-term $\langle \Delta e_{\rm IS} \Delta e_{\rm vib} \rangle$ in figures 3 and 4. Indeed, in the harmonic approximation $e_{\rm vib} = \frac{3}{2} k_{\rm B} T$, and thus it is uncorrelated with $e_{\rm IS}$.

While at low T the harmonic approximation offers a valuable estimate of the basin free energy, on increasing T its validity decreases. A significant breakdown of the approximation is observed close to the onset temperature due to an overcounting of the configurational space volume. Indeed, the configurational space associated with each basin explored in the harmonic approximation (or, to be more precise, the vibrational entropy) is a growing function of T and hence there must exist a temperature at which the volumes of different basins explored overlap.

6.2. Anharmonic basin free energy

Anharmonic corrections can be included in PEL calculations to improve the precision of the calculation of $S_{\rm conf}$. The anharmonic energy $U_{\rm anh}$, defined as

$$U_{\rm anh}(T,V) = U(T,V) - \langle e_{\rm IS} \rangle (T,V) - \tfrac{3}{2} N k_{\rm B} T, \tag{27}$$

can be calculated from the potential energy U and from the average inherent structure energy.

Two possible schemes for the evaluation of the anharmonic vibrational entropy $S_{\rm anh}$ have been proposed for bulk systems[11]. The two approximations are conceptually very different.

In the first case anharmonicity is assumed to be independent of the basin depth and hence the T dependence of $U_{\rm anh}$ can be assumed to be function only of T. The numerical estimate of $U_{\rm anh}$ can be fitted with a polynomial in powers of T starting with T^2:

$$U_{\rm anh}(T,V) = \sum_{i=2}^{i_{\rm max}} c_i(V) T^i. \tag{28}$$

The corresponding anharmonic entropy is

$$S_{\rm anh}(T,V) = \sum_{i=2}^{i_{\rm max}} \frac{c_i(V)}{i-1} T^{i-1}. \tag{29}$$

The present approximation is expected to improve the estimate of the basin entropy if the fit of $U_{\rm anh}$ can be achieved with a small value of $i_{\rm max}$.

In the second case [24, 40], the anharmonicity is assumed to be weak ($i_{\rm max=2}$) but the coefficient c_2 is assumed to be $e_{\rm IS}$ dependent. In this case

$$U_{\rm anh}(T,V) = c_2(e_{\rm IS},V) T^2 \tag{30}$$

[11] A number of different schemes have been tried for including anharmonicity in the study of clusters, such as Haarhof's model, Chekmarev's confinement scheme, short series expansions in T (similar to the one discussed in section 6.2), and also more sophisticated reweighting schemes using quenching, which are related to histogram approaches. Again, we refer the reader to the recent monograph by Wales for a complete review of this important work [11].

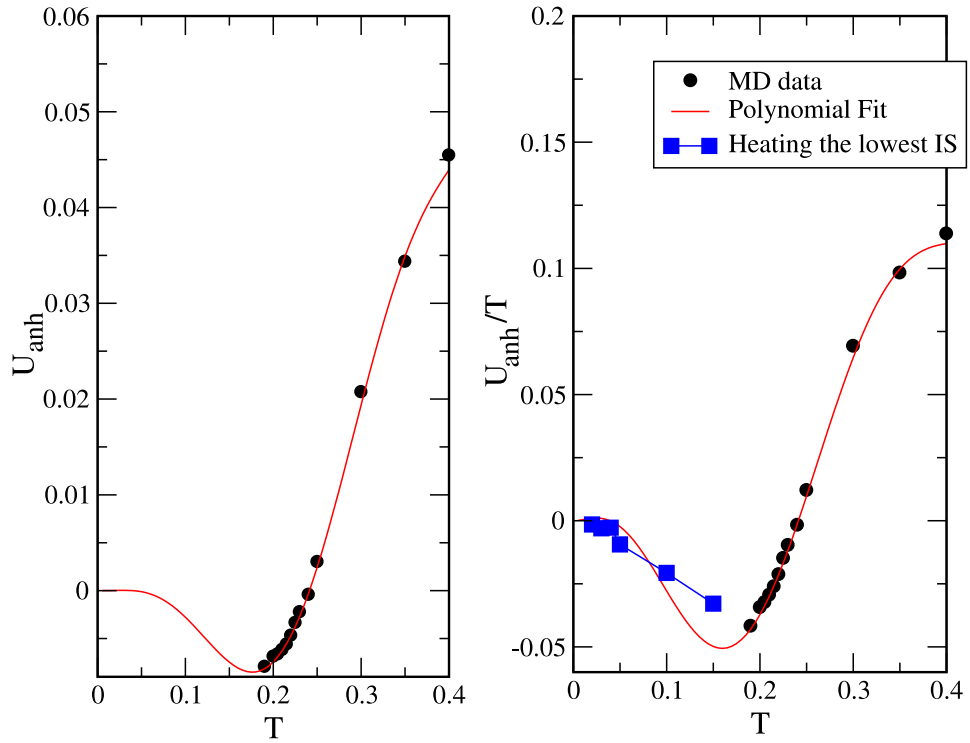

Figure 5. Anharmonic energy for the 50–50 SS binary mixture. The left panel shows the polynomial fit to $U_{\rm anh}$ according to equation (28). The right panel provides convincing evidence that, for the SS case, anharmonic contributions should be handled according to equation (30).

and the corresponding anharmonic entropy is

$$S_{\rm anh}(T,V) = -2c_2(e_{\rm IS},V)T. \tag{31}$$

The function $c_2(e_{\rm IS},V)$ can be calculated by equating equations (27) and (30). A check on the quality of this approximation could in principle be achieved by studying numerically the T dependence of the potential energy on heating an IS configuration. Unfortunately, this test can be performed only for low $e_{\rm IS}$, since only for these deep energy basins does the heating process not involve basin changes.

Figure 5 shows the T dependence of the anharmonic energy for a binary mixture of soft spheres and the fit with equation (28). A large value of $i_{\rm max}$ is required to fit the T dependence, suggesting that this approximation is not appropriate. The right figure shows $e_{\rm anh}/T$ both for the equilibrium data and during heating of the $T = 0.2$ basin. The observed linear dependence of $e_{\rm anh}/T$ and the extrapolation to the equilibrium value strongly support equation (31) as a route for evaluating $S_{\rm anh}$ in soft sphere systems.

6.3. Basin free energy: the square well case

An interesting model, for which the basin free energy can be exactly calculated, is the square well model [41]. Indeed, in this model, an IS configuration is defined in terms of the bonding pattern and the basin of a particular IS consists of all points in configuration

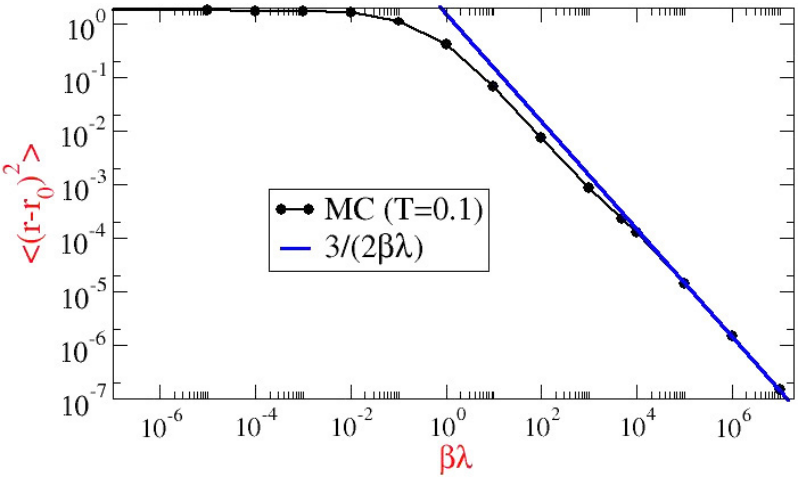

Figure 6. Mean square displacement at $T = 0.1$ for the maximum valency square well model [41] with $N_{\max} = 3$ as a function of λ. The full line shows the harmonic behaviour $\frac{3}{2}(1/\beta\lambda)$.

space sampled by the liquid when no bonds are either created or destroyed. In a Monte Carlo simulation, it is possible to reject all moves associated with bond formation or bond breaking. Since it is not possible to evaluate the Hessian for stepwise potentials, it is not possible to calculate f_{basin} as a sum of a harmonic and an anharmonic free energy. The evaluation of the basin free energy is accomplished by a thermodynamic integration starting from a set of $3N$ Einstein oscillators, i.e. from a system described by a Hamiltonian

$$H^E(\vec{r}^N) = \lambda \sum_i (\vec{r}_i - \vec{r}_i{}^0)^2 \tag{32}$$

where $\vec{r}_i{}^0$ is the IS configuration whose basin free energy needs to be evaluated.

Indicating by H^0 the original square well potential, and performing a series of MC simulations of the Hamiltonian

$$H(\vec{r}^N) = H^0(\vec{r}^N) + \lambda \sum_i (\vec{r}_i - \vec{r}_i{}^0)^2 \tag{33}$$

at fixed T and V (and constrained to satisfy at all steps the IS bonding pattern) for different values of λ, the required basin free energy is provided by thermodynamic integration (in λ) [21], [42]–[44]:

$$f_{\text{vib}}(T,V) = F_{H_E}(T,V,\lambda_{\max}) - \int_0^{\lambda_{\max}} \left\langle \sum_i (\vec{r}_i - \vec{r}_i{}^0)^2 \right\rangle_\lambda \mathrm{d}\lambda \tag{34}$$

where $\langle \sum_i (\vec{r}_i - \vec{r}_i{}^0)^2 \rangle_\lambda$ is the mean square displacement, summed over all particles, at fixed value of λ. Numerically, simulations are performed up to values of $\lambda_{\max}$ for which the Einstein model (whose free energy $F_{H_E}(T,V,\lambda_{\max})$ is analytically known) is recovered. An example of such a calculation is reported in figure 6. At large λ values, the mean square displacement per particle approaches the theoretically expected limit $\frac{3}{2}(1/\beta\lambda)$.

In principle, this technique can be used also for evaluating the basin free energy in continuous potentials [43, 44]. Unfortunately, in these cases, there is no unique way to

constrain the system to explore only the configuration space associated with the starting IS. For small values of λ the system is free to change basin. For this reason, an arbitrary criterion must be selected as the low $\lambda_{\min}$ cut-off. Reasonable choices of $\lambda_{\min}$ can be made by picking the value of λ at which the mean square displacement becomes identical to the plateau location in the unconstrained $\langle r^2 \rangle$.

7. Modelling the statistical properties of the PEL: the Gaussian landscape

The goal of the PEL formalism is to provide a thermodynamic description of supercooled liquid states in terms of statistical properties of the potential energy surface, i.e. the number of basins of different depths and their volume in configuration space. With the technique described above, both types of information become accessible: $S_{\rm conf}$, a measure of the number of basins of depth $e_{\rm IS}$, is calculated as the difference between the liquid entropy and the basin entropy, while the relation between the basin depth and basin volume is estimated via the evaluation of the density of states and, when possible, via the evaluation of the anharmonic contributions. The quality of these estimates makes it possible to compare the numerical results with theoretical models for the statistical properties of the landscape[12].

The model which has been explored most up to the present is the random energy model (REM) [45, 46], which appears to be consistent with the numerical evidence for fragile liquids [36, 39, 47, 48]. The REM is based on the hypothesis that the number $\Omega(e_{\rm IS})\,{\rm d}e_{\rm IS}$ of distinct basins of depth between $e_{\rm IS}$ and $e_{\rm IS} + {\rm d}e_{\rm IS}$ in a system of N atoms or molecules is described by a Gaussian distribution, i.e.,

$$\Omega(e_{\rm IS})\,{\rm d}e_{\rm IS} = {\rm e}^{\alpha N}\frac{{\rm e}^{-(e_{\rm IS}-E_0)^2/2\sigma^2}}{(2\pi\sigma^2)^{1/2}}\,{\rm d}e_{\rm IS}. \tag{35}$$

Here the amplitude ${\rm e}^{\alpha N}$ accounts for the total number of basins, E_0 has the role of the energy scale and σ^2 measures the width of the distribution. One can understand the origin of such a distribution by invoking the central limit theorem. Indeed, in the absence of a diverging correlation length, in the thermodynamic limit, each IS can be decomposed into a sum of independent subsystems, each of them characterized by its own value of $e_{\rm IS}$. The system IS energy, in this case, will be distributed according to equation (35). Note that this hypothesis will break down in the very low energy tail, where differences between the Gaussian distribution and the actual distribution become relevant. As discussed in [47], the system Gaussian behaviour reflects also the Gaussianity of the independent subsystems.

Within the assumptions of equation (35)—Gaussian distribution of basin depths—and the assumption of a quadratic dependence of the basin free energy on $e_{\rm IS}$, an exact evaluation of the partition function can be carried out. The corresponding Helmholtz free energy can be found in [24]. Here, for didactic reasons, I limit myself to the case of linear dependence of the basin free energy on $e_{\rm IS}$, in the harmonic approximation. The partition function for the Gaussian model is

$$Z(T,V) = \int \Omega(e_{\rm IS})\,{\rm d}e_{\rm IS}{\rm e}^{-\beta e_{\rm IS}+f_{\rm vib}(e_{\rm IS},T,V)}. \tag{36}$$

[12] It is worth noting that the PES has been visualized directly using disconnectivity graphs in the region of the global minimum for various bulk models, including LJ, BMLJ and Stillinger–Weber silicon ones [11].

The assumption of linear dependence of $f_{\rm vib}(e_{\rm IS}, T, V)$ on $e_{\rm IS}$ in the harmonic approximation corresponds to the case (see equation (26))

$$\mathcal{S}(e_{\rm IS}) = a(V) + b(V)e_{\rm IS}. \tag{37}$$

The coefficients a and b can be calculated numerically, for each model, by fitting $\mathcal{S}(e_{\rm IS})$. The resulting vibrational free energy can be written as

$$f_{\rm vib}(e_{\rm IS}, T, V) = f_{\rm vib}(E_0, T, V) - k_{\rm B}Tb(V)(e_{\rm IS} - E_0) \tag{38}$$

and the Helmholtz free energy as

$$\begin{aligned} F(T,V) = &-TS_{\rm conf}(T,V) + \langle e_{\rm IS}(T,V)\rangle + f_{\rm vib}(E_0,T,V) \\ &- k_{\rm B}Tb(V)(\langle e_{\rm IS}(T,V)\rangle - E_0(V)). \end{aligned} \tag{39}$$

The corresponding T dependences of $\langle e_{\rm IS}(T,V)\rangle$ and $S_{\rm conf}$ are

$$\langle e_{\rm IS}(T,V)\rangle = E_0(V) - b(V)\sigma^2 - \beta\sigma^2(V) \tag{40}$$

and

$$S_{\rm conf}(T,V)/k_{\rm B} = \alpha(V)N - \frac{(\langle e_{\rm IS}(T,V)\rangle - E_0(V))^2}{2\sigma^2(V)}. \tag{41}$$

The Gaussian PEL predicts the existence of a finite T, named $T_{\rm K}$ in honour of Kauzmann [6], at which $S_{\rm conf} = 0$. Below $T_{\rm K}$ the system remains trapped in this low energy basin with energy $e_{\rm K}$ and its free energy coincides with the basin free energy. In terms of Gaussian PEL parameters, $T_{\rm K}$ and $e_{\rm K}$ are given by

$$\begin{aligned} e_{\rm K} &= E_0 - \sqrt{2\alpha N}\sigma \\ kT_{\rm K} &= \left(\sqrt{\frac{2\alpha N}{\sigma^2}} - b\right)^{-1}. \end{aligned} \tag{42}$$

Note that, in the harmonic Gaussian approximation, from a plot of $\langle e_{\rm IS}(T)\rangle$ versus $1/T$, two of the parameters of the Gaussian distribution, σ^2 (from the slope) and E_0 (from the intercept), can be evaluated. Similarly, from fitting $S_{\rm conf}(T)$ according to equation (41), one can evaluate the parameter α.

The fitting parameters $\alpha(V)$, $E_0(V)$ and $\sigma^2(V)$ depend in general on the volume. A study of the volume dependence of these parameters, associated with the V dependence of the shape indicators ($a(V)$ and $b(V)$ in equation (37)), provides a full characterization of the volume dependence of the landscape properties of a model, and offers the possibility of developing a full equation of state based on statistical properties of the landscape.

When comparing numerical simulation data and theoretical predictions—equations (40) and (41)—the range of temperatures must be chosen with great care. Indeed, at high T, the harmonic approximation will overestimate the volume in configuration space associated with an inherent structure. While in the harmonic approximation such a quantity is unbounded, the real basin volume is not. Indeed, the sum of all basin volumes is equal to the volume of the system in configuration space. Anharmonic corrections, if properly handled, should compensate such overestimate, but at the present time, no model has been developed for correctly describing the high T limit of the anharmonic

J. Stat. Mech. (2005) P05015

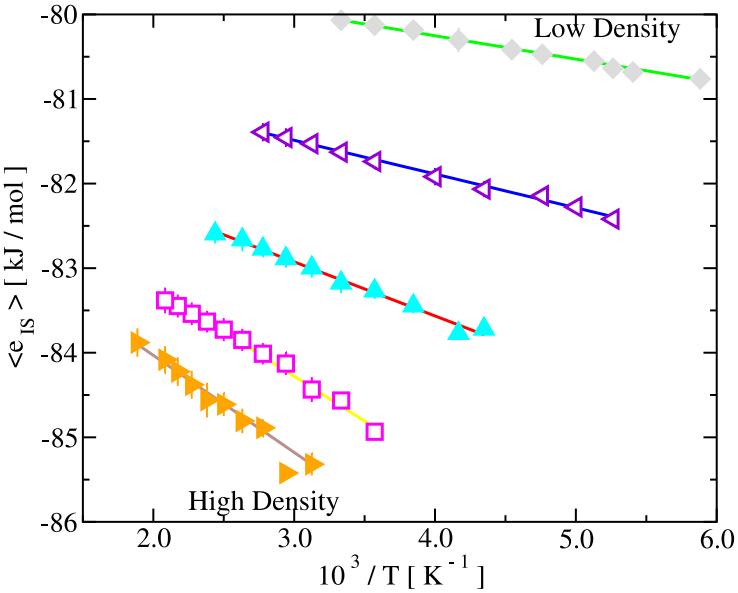

Figure 7. Temperature dependence of the IS energy for the LW-OTP model for five different densities. In all cases, a $1/T$ dependence, consistent with a Gaussian landscape, is observed.

component. Numerical studies have shown that the range of validity of the present estimates of the anharmonic correction does not extend beyond the temperatures at which the system already shows a clear two-step relaxation behaviour in the dynamics. Indeed, the presence of a two-step relaxation is a signature of the system spending a time larger than the microscopic characteristic time around a well defined local minimum. Support for the harmonic Gaussian approximation comes from a series of studies based on fragile liquids. Figure 7 shows the T dependence of $\langle e_{\rm IS}(T,V)\rangle$ for the case of the LW-OTP model. Similar results have been obtained for SPC/E water and BMLJ cases. Less convincing is the case of SS, where anharmonic corrections play a relevant role (see figure 5).

Figure 8 shows the comparison of the Gaussian prediction for the configurational entropy, both in $e_{\rm IS}$ and in T, for the BMLJ case. If the Gaussian model were to hold even beyond the region of T or $e_{\rm IS}$ where numerical equilibrium data are available, $S_{\rm conf}$ would vanish at a finite T, which defines $T_{\rm K}$ and $e_{\rm K}$ for the model.

Another test of the harmonic Gaussian model can be carried out when a large number of IS have been generated for each T. In this case, it becomes possible to study the distribution $P(e_{\rm IS},T)$ [23, 39, 51] of energies sampled at a given temperature. In the Gaussian harmonic approximation, this distribution is a Gaussian, with a T independent variance [52]. Indeed,

$$P(e_{\rm IS},T)=\frac{\Omega(e_{\rm IS})\mathrm{e}^{-\beta e_{\rm IS}+f_{\rm vib}(e_{\rm IS},T)}}{Z(T,V)}. \tag{43}$$

In the harmonic approximation $\beta f_{\rm vib}$ can be written as

$$\beta f_{\rm vib}(e_{\rm IS},V)=-3N\ln(\beta)-\left\langle\sum_j^{3N}\ln[\hbar\omega_j]\right\rangle_{e_{\rm IS}}=-3N\ln(\beta)-3N(a+be_{\rm IS}) \tag{44}$$

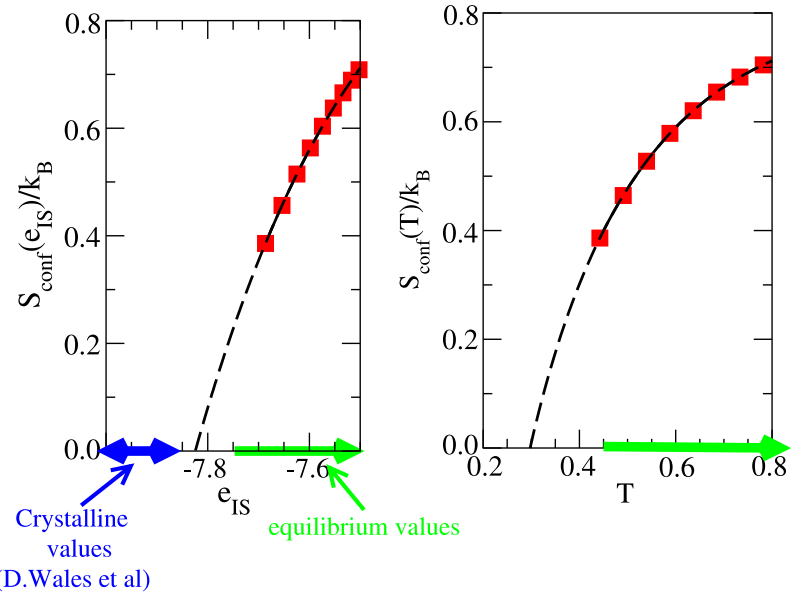

Figure 8. IS energy (left) and temperature (right) dependences of the configurational entropy for the BMLJ model. The full lines extrapolate to $S_{\rm conf} = 0$ at the Kauzmann energy $e_{\rm K}$ and the Kauzmann temperature $T_{\rm K}$. The arrow indicates the range of energy values of the crystal [49, 50].

where use has been made of equation (37). Hence, $P(e_{\rm IS}, T)$ results in [52]

$$P(e_{\rm IS}, T) = \frac{\exp\Big(-(e_{\rm IS} - \langle e_{\rm IS}(T,V)\rangle)^2/2\sigma^2\Big)}{\sqrt{2\pi\sigma^2}}. \tag{45}$$

The evaluation of $P(e_{\rm IS}, T)$ offers also an alternative procedure for estimating $S_{\rm conf}(e_{\rm IS})$ for the harmonic vibrational free energies [53]. Indeed, the quantity $\ln[P(e_{\rm IS}, T)] + \beta e_{\rm IS}$ is only a function of $e_{\rm IS}$ times an unknown multiplicative T dependent factor. Curves obtained at different T can be superimposed according to the histogram reweighting techniques to generate a vibrationally weighted $\Omega(e_{\rm IS})$, as shown in figure 9. In the case of equal shape basins ($b = 0$ in equation (37)) the resulting histogram coincides with $S_{\rm conf}(e_{\rm IS})$.

7.1. Potential energy landscape equation of state: the Gaussian harmonic landscape

In the case of the Gaussian harmonic landscape it is possible to derive an expression for the equation of state $P(T, V)$ fully based on PEL properties [48]. Indeed, $P(T, V) = -(\partial F(T, V)/\partial V)|_T$. The volume derivative of equation (12) involves only the landscape parameters α, σ^2, E_0 and b. The resulting expression for P can be written as

$$P(T, V) = \mathcal{P}_{\rm const} + T\mathcal{P}_T + T^{-1}\mathcal{P}_{1/T}, \tag{46}$$

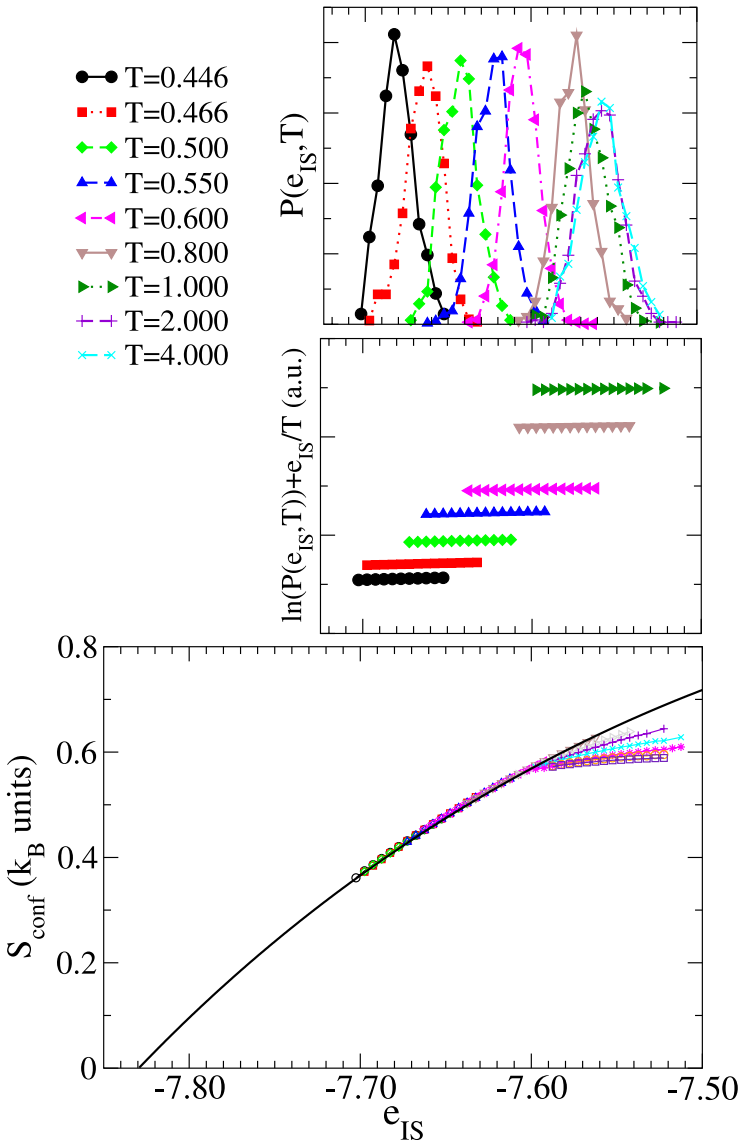

Figure 9. Evaluation of the (vibrationally weighted [53, 54]) configurational entropy for the BMLJ model. Note that for $T < 0.8$, curves for different T can be scaled onto a master plot, which provides an estimate of the $e_{\rm IS}$ dependence of the configurational entropy (redrawn from [23, 53]).

where

$$\mathcal{P}_{\rm const}(V) = -\frac{\mathrm{d}}{\mathrm{d}V}\left[E_0 - b\sigma^2\right]$$
$$\mathcal{P}_T(V) = R\,\frac{\mathrm{d}}{\mathrm{d}V}\left[\alpha - a - bE_0 + b^2\sigma^2/2\right] \qquad (47)$$
$$\mathcal{P}_{1/T}(V) = \frac{\mathrm{d}}{\mathrm{d}V}\left[\sigma^2/2R\right].$$

Stability at high T implies that $\mathcal{P}_T$ must be positive. The case $b = 0$ helps in clarifying the landscape origin of the three contributions. The T independent constant term $\mathcal{P}_{\rm const}$

originates from the volume dependence of the energy scale of the system E_0. The linear term $T\mathcal{P}_T$ arises from the entropic contribution encoded in the V derivative of the total number of states per particle α and the vibrational contribution associated with the change of the density of states with V. Finally, the low T dominant $\mathcal{P}_{1/T}/T$ term has an entropic origin, related to changes in the numbers of states explored.

Along an isochore, the high T behaviour is fixed by the linear term $T\mathcal{P}_T > 0$, while the low T behaviour is controlled by the T^{-1} term $T^{-1}\mathcal{P}_{1/T}$. From equation (46) one can also conclude that in the harmonic Gaussian landscape the pressure along an isochore either is monotonically increasing with T (if $\mathcal{P}_{1/T} \leq 0$) or has a minimum (as found in the case of liquids with density anomalies [38]) at $T = \sqrt{\mathcal{P}_{1/T}(V)/\mathcal{P}_T(V)}$ (if $\mathcal{P}_{1/T} > 0$).

Equation (46) offers the possibility of understanding the landscape parameters responsible for density anomalies [38]. Indeed, a Maxwell relation states that a density maximum state point (i.e. a point where $\partial V/\partial T|_P = 0$) is simultaneously a point at which the T dependence of the pressure along an isochore has a minimum ($\partial P/\partial T|_V = 0$). Hence, the condition for the existence of density maxima, from equation (46), is that $P_{1/T}(V) > 0$ which, in the PEL formalism, corresponds to $\mathrm{d}\sigma^2/\mathrm{d}V > 0$. Thus, the landscape property which determines the anomalous density behaviour is the V dependence of σ^2. Anomalous behaviour can be found only within a region of volumes where σ^2 increases with V, delimited by the V at which $\mathrm{d}\sigma^2/\mathrm{d}V = 0$. In passing, we also note that the structure of equation (46) suggests that, in the harmonic Gaussian landscape, density minima (maxima in isochoric $P(T)$) cannot be present.

7.2. Gaussian landscape in soft spheres

The volume dependence of the landscape parameters, under the assumption of a Gaussian PEL, can be calculated analytically for the case of the soft sphere potential [55]–[58]. The self-similar nature of the potential $V(r) \sim \epsilon(\sigma/r)^n$ implies that βF^{ex}, the free energy in excess of the ideal gas free energy, is a function of the scaling variable $\gamma \equiv TV^{n/3}$ [59]. In the landscape formalism, this means that $\beta\langle e_{\mathrm{IS}}\rangle$ and S_{conf} must be functions of γ, as well as the excess basin free energy. Looking at equations (40) and (41) one immediately sees that in the case of a Gaussian PEL,

$$\begin{aligned} E_0 &\sim V^{-n/3} \\ \sigma^2 &\sim V^{-2n/3} \\ \alpha &\sim V^0. \end{aligned} \tag{48}$$

Similar calculations show that, in the harmonic approximation, normal model frequencies scale as

$$\omega_i^2 \sim V^{-(n+2)/3}. \tag{49}$$

For the case of SS, some other interesting relations can be derived from the self-similarity of the potential. In particular, isotropic compression of an IS SS configuration always leaves the system in a minimum. The energy of the minimum scales with volume as $e_{\mathrm{IS}} \sim V^{-n/3}$ and, hence, the pressure experienced in the IS configuration is simply given by

$$P_{\mathrm{IS}} = -\frac{\mathrm{d}e_{\mathrm{IS}}}{\mathrm{d}V} = \frac{n}{3}\frac{e_{\mathrm{IS}}}{V}. \tag{50}$$

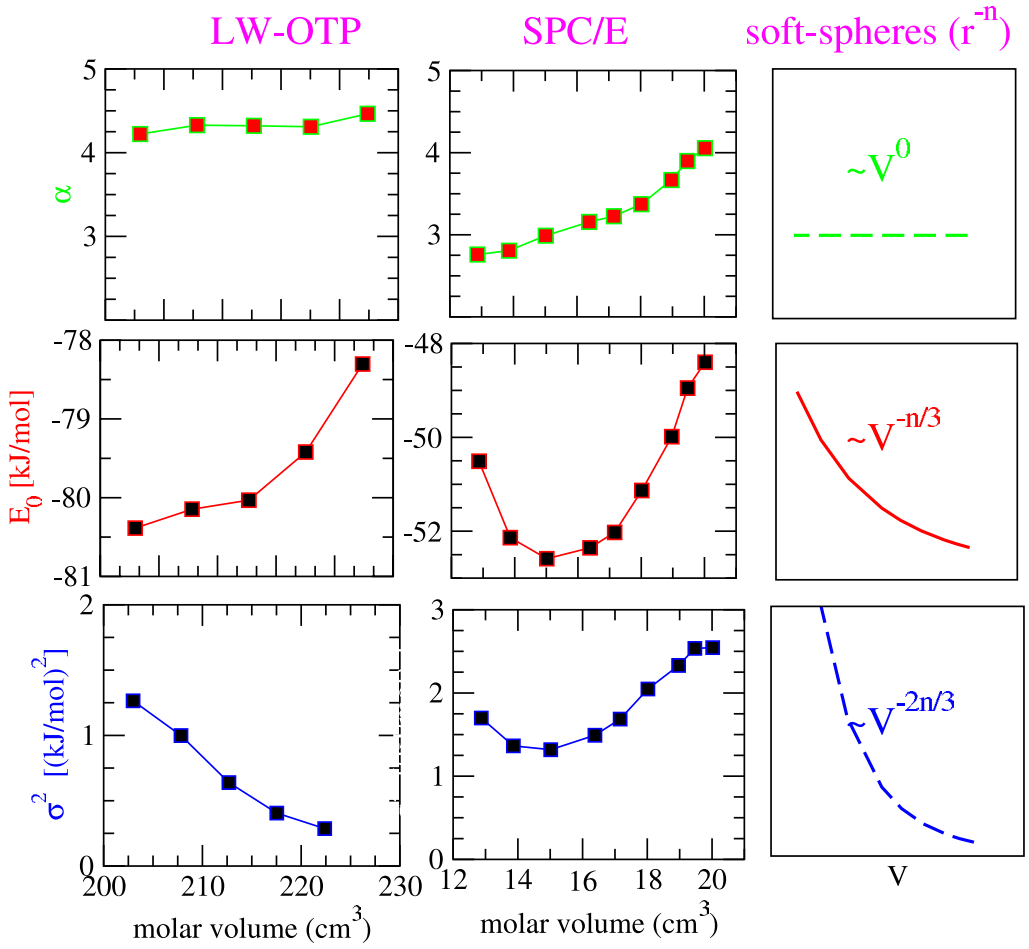

Figure 10. Volume dependence of the parameters α, E_0 and σ^2 for SPC/E, LW-OTP and SS cases. Note that in the case of SPC/E water, a region of volumes exists where $\partial\sigma^2/\partial V > 0$, the PEL indicator of density anomalies [38].

The contribution to P arising from the harmonic vibrational degrees of freedom can also be estimated from the scaling relation in equation (49). Indeed,

$$P_{\rm vib} = -\frac{\partial f_{\rm vib}}{\partial V} = kT\frac{\partial \sum_i^{3N} \ln[\beta\hbar\omega_i]}{\partial V} = 3N\frac{n+2}{6}\frac{kT}{V}. \tag{51}$$

As a result, for the soft sphere case, in the harmonic approximation, the EOS can be written as[13]

$$P = P_{\rm IS} + P_{\rm vib} = \frac{n}{3}\frac{e_{\rm IS}}{V} + \frac{n+2}{2}\frac{NkT}{V}. \tag{52}$$

[13] The same relation can be derived in a standard approach by remembering that in self-similar potential, the excess pressure $P^{\rm ex}$ and potential energy E are related by $P = (n/3)E/V$. This expression can be read as the fact that isotropic compression changes only the potential energy and does not touch the excess entropy of the system. By adding the ideal gas contribution to the pressure and writing, in the harmonic approximation, $E = e_{\rm IS} + \frac{3}{2}NkT$, one recovers $PV = (n/3)e_{\rm IS} + ((n+2)/2)NkT$.

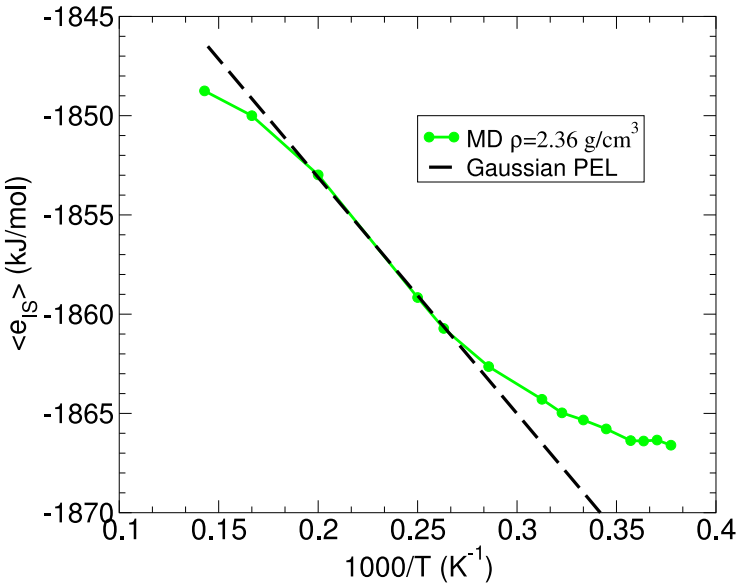

Figure 11. Temperature dependence of $\langle e_{\rm IS}\rangle$ for BKS silica. The $1/T$ law characteristic of Gaussian landscapes is observed only in a restricted region of temperatures. Redrawn from [62].

7.3. Volume dependence of α, E_0, σ^2

The volume dependences of the landscape parameters have been studied numerically for the BMLJ [39], SPC/E [38] and LW-OTP [19, 48] models. In the case of soft spheres (see equation (48)) the self-similar nature of the interaction potential fixes the volume dependence of the landscape parameters.

Figure 10 shows the V dependence of the Gaussian PEL parameters for LW-OTP, SPCE/E and SS cases. For these continuous potentials, the total number of states per particle α is weakly dependent on V, slightly increasing with increasing V. The energy scale E_0, which is monotonically decreasing in SS, has a minimum in both SPC/E and LW-OTP cases, as expected from the balance between attractive and repulsive energies. The variance σ^2 is monotonically decreasing in SS and LW-OTP cases. In the SPC/E case it shows the expected range of volumes where $\mathrm{d}\sigma^2/\mathrm{d}^2V > 0$, the harmonic Gaussian landscape signature of density anomalies.

8. Landscape of strong liquids

The statistical properties of a landscape for strong liquids are a topic of current investigation. In the case of BKS silica, whose PEL properties have been investigated [60]–[65], there is clear evidence that at low T, the distribution of IS energies significantly deviates from the Gaussian one [62]. The breakdown of the Gaussian approximation is extremely clear in the T dependence of $\langle e_{\rm IS}(T,V)\rangle$ (figure 11) which approaches a constant value at low T and from the analogous effect in $S_{\rm conf}$ (figure 12) [62, 64]. $S_{\rm conf}$ does not appear to extrapolate to zero at a finite T, suggesting the absence of a finite Kauzmann T in this model. The deviation from Gaussian behaviour has been recently connected

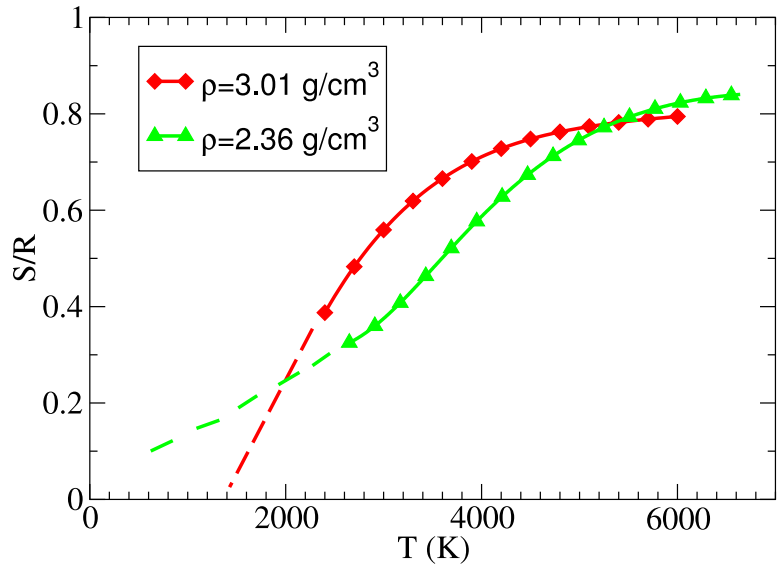

Figure 12. T dependence of $S_{\rm conf}$ for BKS silica at $\rho = 2.36$ and 3.01 g cm^{-3}. Note that in this model, at the lowest density, $S_{\rm conf}$ does not appear to vanish at a finite T. Dashed lines represent possible extrapolations. Redrawn from [62].

to the progressive formation of a defect free tetrahedral network which acts as a ground state for the system [65]. Support for this interpretation has recently been provided from the landscape analysis of a maximum valency model [41], which identifies in the finite degeneracy of the ground state and in the logarithmic distribution of $\Omega(e_{\rm IS})$ close to the ground state the key ingredients of the landscape of strong liquids. It is also interesting to observe that the breakdown of the $1/T$ dependence in $\langle e_{\rm IS}\rangle(T, V)$ takes place at T which the dynamics of BKS silica crosses from super-Arrhenius to Arrhenius [66]. The search for an accurate model for the landscape of strong liquids is a current topic of research and we expect significant developments in the next few years.

9. Ageing in the PEL formalism: thermodynamics with one additional effective parameter

The PEL framework is particularly suited for describing out-of-equilibrium conditions. As seen previously, the system is represented by its $e_{\rm IS}$ energy, independently from thermodynamic conditions. The system is said to be in equilibrium at T if $e_{\rm IS}$ is, within fluctuations, equal to $\langle e_{\rm IS}\rangle(T)$. If $e_{\rm IS}$ is different from $\langle e_{\rm IS}\rangle(T)$, a time evolution of $e_{\rm IS}$ takes places. I will call this process an out-of-equilibrium (ageing) dynamics. I will not discriminate between conditions where thermal equilibrium can never be reached (a liquid to glass transformation) and conditions where, within our observation time window, final equilibration can be achieved (liquid to liquid, glass to liquid transformations)[14].

[14] In theoretical studies of out-of-equilibrium conditions, asymptotic results are often derived for $t_{\rm w} \to \infty$. The word *ageing* is limited to use in cases in which, even at infinite time, the system is out of equilibrium. Hence, in some studies glass to liquid and liquid to liquid transformations do not qualify for the description of 'ageing'.

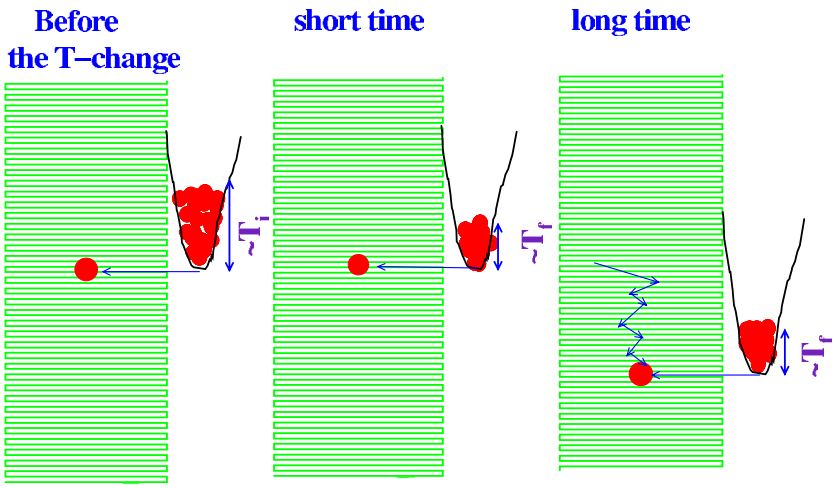

Figure 13. Schematic representation of the ageing process in the PEL framework. Before the T quench, the system is in equilibrium, exploring basins of the landscape with appropriate energy (left panel). At short times after the quench (middle panel), the vibrational degrees of freedom thermalize to T_f, but the system has not changed basin. For longer times (right panel), the system explores deeper and deeper basins, but with his vibration properties fixed by T_f.

Consider a system in equilibrium at a starting T_i which is suddenly coupled to a thermostat with a final temperature T_f. The hypothesis of a clear separation between fast intrabasin dynamics and slow interbasin dynamics is equivalent to stating that after the T change the vibrational degrees of freedom thermalize immediately to the new bath temperature T_f. At short times, the system is confined in the original basin but the exploration of the basin (the vibrational component) is now controlled by T_f. If $T_\mathrm{f} < T_\mathrm{i}$, during the ageing dynamics, the system explores progressively deeper and deeper basins until it reaches basins with depth consistent with the equilibrium expected value $\langle e_\mathrm{IS}(T_\mathrm{f})\rangle$. During ageing, the vibrational component is always fixed by T_f. A schematic representation of ageing on the PEL is provided in figure 13, where the location of the system on the landscape is represented before the T quench (left), a short time after the T quench (middle) and for longer time (right) when the exploration of the landscape is taking place. It is important to point out that this idea of interpreting the ageing dynamics in terms of motion of the landscape requires an apparently inoffensive hidden hypothesis, i.e. the fact that the distribution of levels, rebuilt from the analysis of equilibrium configurations, is identical to the one explored during the ageing dynamics. In other words, the basins explored in the ageing dynamics are assumed to be identical to the ones explored in equilibrium, not only in their average properties but also in their intrinsic inhomogeneities (fluctuations).

Figure 14 shows, for the BMLJ case, the evolution of $\langle e_\mathrm{IS}(t_\mathrm{w})\rangle$ as a function of the time t_w elapsed from the T quench. One can see that $\langle e_\mathrm{IS}(t_\mathrm{w})\rangle$ decreases with a logarithmic time dependence. Following the theoretical work developed for the ageing of disordered p-spin models [67]–[69], one can attempt to develop a thermodynamic description of the ageing system within the PEL framework. The idea is to evaluate the partition function of the system, from the known distribution of IS basins, under the constraint that the

J. Stat. Mech. (2005) P05015

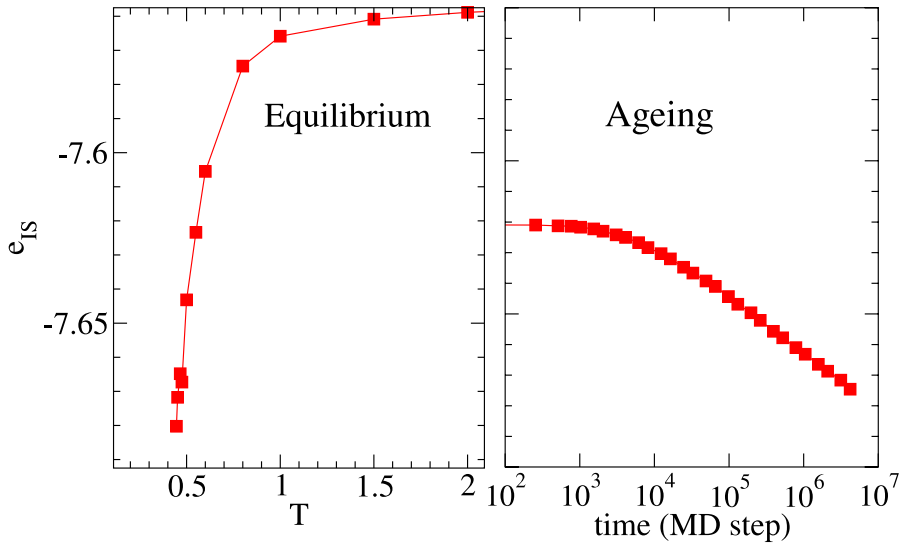

Figure 14. Left: equilibrium T dependence of $e_{\rm IS}$ for the BMLJ model. Right: waiting time dependence of $e_{\rm IS}$ following a T quench from $T = 0.55$ to 0.3.

basin free energy is fixed by the bath temperature (which we call T in the following). With this hypothesis, we can write the system partition function as

$$Z(T_{\rm eff}, T, V) = \sum_{e_{\rm IS}} \Omega(e_{\rm IS}) {\rm e}^{-\beta_{\rm eff} f_{\rm basin}(e_{\rm IS}, T, V)} \tag{53}$$

where an unknown $\beta_{\rm eff} \equiv 1/kT_{\rm eff}$ is introduced to account for the out-of-equilibrium conditions. When $\beta_{\rm eff} = \beta$, equilibrium conditions are restored. The resulting free energy can be calculated by finding the solution of the equation

$$T_{\rm eff} \frac{\partial S_{\rm conf}(e_{\rm IS})}{\partial e_{\rm IS}} - \frac{\partial f_{\rm basin}(e_{\rm IS}, T, V)}{\partial e_{\rm IS}} = 1. \tag{54}$$

Differently from the equilibrium case, where T and V are fixed and $e_{\rm IS}(T, V)$ is unknown, in the case of ageing, we assume that we know, beside the bath T and V, also the basin in which the system is located at $t_{\rm w}$ (i.e. the $e_{\rm IS}$ value) and we search for the $T_{\rm eff}$ solution of the above equation[15]. The resulting expression for $T_{\rm eff}$ is

$$T_{\rm eff} = \frac{\partial f_{\rm basin}(e_{\rm IS}, T, V)/\partial e_{\rm IS}}{\partial S_{\rm conf}(e_{\rm IS})/\partial e_{\rm IS}} \tag{55}$$

or, by using the equilibrium expression for $\partial S_{\rm conf}(e_{\rm IS})/\partial e_{\rm IS}$ from equation (11),

$$T_{\rm eff} = \frac{\partial f_{\rm basin}(e_{\rm IS}, T)/\partial e_{\rm IS}}{\partial f_{\rm basin}(e_{\rm IS}, T_{\rm eq})/\partial e_{\rm IS}} T_{\rm eq} \tag{56}$$

[15] It may help to think of the thermodynamic approach to OOE systems in terms of the microcanonical ensemble. Indeed, if we neglect for a moment the vibrational contributions, what we are doing is assuming knowledge of the energy of the system ($e_{\rm IS}$) and assuming that the system cannot change its energy (due to the fact that relaxation processes are extremely slow) but it can equilibrate among different basins with the same $e_{\rm IS}$. Under these assumptions, what we are essentially writing out are the microcanonical expressions for T at fixed energy. The presence of non-zero vibrational contributions only makes the formalism a little bit more complicated; it does not change the basic meaning.

doi:10.1088/1742-5468/2005/05/P05015

J. Stat. Mech. (2005) P05015

where we have indicated by $T_{\rm eq}$ the temperature at which, *in equilibrium*, the basin $e_{\rm IS}$ is explored. To get a better grasp of the meaning of $T_{\rm eff}$ one can consider the simple case of a PEL where all basins have identical volume (i.e. basin shape independent from the basin depth). In this simple case, the only basin free energy difference arises from the basin depth and $\partial f_{\rm basin}(e_{\rm IS},T)/\partial e_{\rm IS} = \partial e_{\rm IS}/\partial e_{\rm IS} = 1$. Hence $T_{\rm eff} = T_{\rm eq}$. In this simple case, the effective temperature coincides with the temperature at which in equilibrium the basin of depth $e_{\rm IS}$ is explored, providing a direct meaning for the concept of effective temperature.

According to the approach outlined, in out-of-equilibrium conditions the system free energy can be written as

$$F(T_{\rm eff},T,V) = -T_{\rm eff}S_{\rm conf}(e_{\rm IS}) + f_{\rm basin}(e_{\rm IS},T,V). \tag{57}$$

The additional parameter $T_{\rm eff}$ provides an indication of the region of configuration space explored by the ageing system. During the ageing dynamics, the system will slowly explore regions of the landscape of lower and lower depth.

It is instructive to look at the energetic and entropic balance during ageing. For simplicity, I focus on the case of basins of identical shape (i.e. $\partial f_{\rm basin}/\partial e_{\rm IS} = 1$). From an energetic point of view, during ageing the system evolves from $e_{\rm IS}$ to $e_{\rm IS} - {\rm d}e_{\rm IS}$, with ${\rm d}e_{\rm IS} > 0$. From an entropic point of view, the system decreases its entropy, going from $S_{\rm conf}(e_{\rm IS})$ to $S_{\rm conf}(e_{\rm IS} - {\rm d}e_{\rm IS})$, which from the definition of $T_{\rm eff}$ (equation (55)) can be written as

$${\rm d}S_{\rm conf} = -\frac{\partial S_{\rm conf}}{\partial e_{\rm IS}}\,{\rm d}e_{\rm IS} = -\frac{{\rm d}e_{\rm IS}}{T_{\rm eff}}. \tag{58}$$

The reservoir, at bath temperature T, absorbs the energy ${\rm d}e_{\rm IS}$, giving rise to a positive entropy change ${\rm d}S_{reservoir} = {\rm d}e_{\rm IS}/T$. The reservoir + liquid entropy change in the elementary ageing process is the positive quantity $-({\rm d}e_{\rm IS}/T_{\rm eff}) + {\rm d}e_{\rm IS}/T$, in agreement with the second law of thermodynamics [70].

This ageing dynamics is associated with a progressive decrease of $T_{\rm eff}$. A complete understanding of the ageing dynamics requires the prediction of $T_{\rm eff}(t_{\rm w})$, a goal far beyond the current state of the art. As the landscape analysis discussed before for the equilibrium case does not provide an indication of the T dependence of the dynamics, here the thermodynamic formalism for out-of-equilibrium liquids does not allow us to predict dynamic information—only static properties at a fixed $t_{\rm w}$ value, once $e_{\rm IS}$ or equivalently $T_{\rm eff}$ is known.

9.1. An example: 'classical' para-hydrogen and ortho-hydrogen

A simple case to study for obtaining a better grasp of the concept of $T_{\rm eff}$ is offered by a classical version of para-hydrogen and ortho-hydrogen, viewed here as a model of a system composed of two different basins. To do this, we condense the combination of nuclear spin statistics with the rotational partition function and the allowed rotational quantum numbers which generate the two hydrogen configurations into differences in basin shapes. In equilibrium, at each T, there is a precise ratio between the two possible configurations of hydrogen. In reality, conversion from para-hydrogen to ortho-hydrogen or vice versa—which we model as the change of basin—is extremely slow and requires the presence of a catalyst. Out-of-equilibrium conditions may last for extremely long times.

In this example, we model this system (classically!) with two basins, one for the ortho-hydrogen and one for the para-hydrogen configurations. We assume that each basin has its own depth and its own curvature.

The partition function Z for the system can be written as $Z = Z_{\rm para} + Z_{\rm ortho}$, summing the partition functions of the two configurations. Assuming classical harmonic basin free energies, indicating by $e_{\rm IS_{para}}$ the IS energy and $\omega^2_{j_{\rm para}}$ the curvature along the jth eigenmode, one can write

$$Z_{\rm para} = \frac{{\rm e}^{-\beta e_{\rm IS_{para}}}}{\prod_j \beta\hbar\omega_{j_{\rm para}}} \tag{59}$$

and a similar expression for $Z_{\rm ortho}$. The probability P of finding, in equilibrium, hydrogen in the para-configuration or ortho-configuration is given by

$$\frac{P_{\rm para}}{P_{\rm ortho}} = \frac{Z_{\rm para}}{Z_{\rm ortho}} = {\rm e}^{-\beta(e_{\rm IS_{para}} - e_{\rm IS_{ortho}})(1-k_{\rm B}Tb)} \tag{60}$$

where we have defined

$$b = \frac{\sum_j \ln[\omega_{j_{\rm para}}/\omega_{j_{\rm ortho}}]}{e_{\rm IS_{para}} - e_{\rm IS_{ortho}}}. \tag{61}$$

Note that $1 - k_{\rm B}Tb$ plays the role of discrete version of $\partial f_{\rm basin}(e_{\rm IS}, T)/\partial e_{\rm IS}$.

Next we change the bath temperature to $T_{\rm bath}$ and assume that, while collisions are not very effective for converting configurations, they succeed in thermalizing vibration. We can then ask ourselves which is the effective temperature we have to use if, with the vibrational statistical weight controlled by $T_{\rm bath}$, the ratio $P_{\rm para}/P_{\rm ortho}$ is the same as the one in equilibrium at temperature $T_{\rm eq}$, just before the quench.

To predict the same ratio $P_{\rm para}/P_{\rm ortho}$ one has to impose that

$$\beta_{\rm eff}(1 - k_{\rm B}T_{\rm bath}b) = \beta_{\rm eq}(1 - k_{\rm B}T_{\rm eq}b) \tag{62}$$

which gives

$$T_{\rm eff} = \frac{(1 - k_{\rm B}T_{\rm bath}b)}{(1 - k_{\rm B}T_{\rm eq}b)} T_{\rm eq} \tag{63}$$

in agreement with the general expression in equation (55).

10. OOE equation of state

If the thermodynamic generalization of equation (57) is meaningful, its volume derivative must provide a measure of the pressure experienced by the ageing system. Since the free energy is now a function of T, V and $T_{\rm eff}$, the EOS can be formally written as

$$P(T_{\rm eff}, T, V) = -\left.\frac{\partial F(T_{\rm eff}, T, V)}{\partial V}\right|_{T,T_{\rm eff}} \tag{64}$$

or

$$P(T_{\rm eff}, T, V) = T_{\rm eff}\left.\frac{\partial S_{\rm conf}(e_{\rm IS})}{\partial V}\right|_{T,T_{\rm eff}} - \left.\frac{\partial f_{\rm basin}(e_{\rm IS}, T, V)}{\partial V}\right|_{T,T_{\rm eff}}. \tag{65}$$

doi:10.1088/1742-5468/2005/05/P05015

J. Stat. Mech. (2005) P05015

This expression, providing a formal link between P and $T_{\rm eff}, T, V$, shows also that, by inversion of the expression, it is possible to define $T_{\rm eff}$ as $T_{\rm eff}(P, T, V)$. In equilibrium, the EOS can be inverted providing a relation $T(P, V)$ which allows us to predict that two systems with the same P and V *are* two realizations of the *same* thermodynamic state point, having the same T. The OOE EOS can also be inverted to predict that two OOE systems, with the same P, T and V, have the same $T_{\rm eff}$ and hence are thermodynamically identical. The history dependence is coded in just one parameter, $T_{\rm eff}$. In the present formalism, two systems, under the same external conditions (same T, V and P), even if they have different thermal histories, have the same $T_{\rm eff}$ and hence are identical.

10.1. Inherent structure pressure

An additional insight into the expression for the free energy of an OOE system is provided by the concept of IS pressure, $P_{\rm IS}$, i.e. of the pressure experienced by the system in the IS configuration. Generally, $P_{\rm IS}$ can always be calculated by evaluating the change in potential energy with volume, on performing an infinitesimal isotropic scaling of the coordinates. This definition of pressure of a configuration is equivalent to the virial expression, commonly used in simulations, and it is not limited to configurations which are local minima of the landscape. In most models for liquid, an infinitesimal compression of an IS configuration moves the system out from the minimum and hence the change in potential energy does not coincide with the change in $e_{\rm IS}$.

To provide an expression for $P_{\rm IS}$ within the PEL approach, we recall that an IS can be considered as the $T = 0$ K glass associated with a liquid state configuration. Interpreting the steepest descent path as a quench to $T = 0$ K, $P_{\rm IS}$ can be identified with the expression provided in equation (65), setting the bath T to zero, i.e. $P_{\rm IS} = P(T_{\rm eff}, 0, V)$. Using the OOE thermodynamic formalism derived above, it is possible to show that $P_{\rm IS}$ is given by [55, 56]

$$P_{\rm IS}(V, e_{\rm IS}) = -\left.\frac{\partial e_{\rm IS}}{\partial V}\right|_{S_{\rm conf}}. \tag{66}$$

It is interesting to note that the calculation of $P_{\rm IS}$ requires an infinitesimal change of V at constant configurational entropy, confirming that $P_{\rm IS}$ does not coincide with $-\partial e_{\rm IS}/\partial V$ on an isotropic scaling of the system.

In the case of the soft sphere model, the validity of equation (66) can be satisfactorily tested. Indeed, for this model an isotropic scaling of the coordinates applied to an IS configuration leaves the scaled system in an IS configuration, due to the self-similarity of the interaction potential. Minima remain minima under isotropic scaling. In all other potentials, minima disappear or appear under coordinate scaling [13]. The self-similar properties of the potential are also responsible for the self-similar nature of the PEL. As a consequence, isotropic compression is, by construction, a constant configurational entropy path. These two properties prove that equation (65), derived from the OOE formalism, is the correct expression, at least for the soft sphere potential.

11. Numerical test of the OOE approach

The quantification of the statistical properties of the PEL sampled by the equilibrium liquid at different volumes is the key feature for developing a landscape thermodynamic

J. Stat. Mech. (2005) P05015

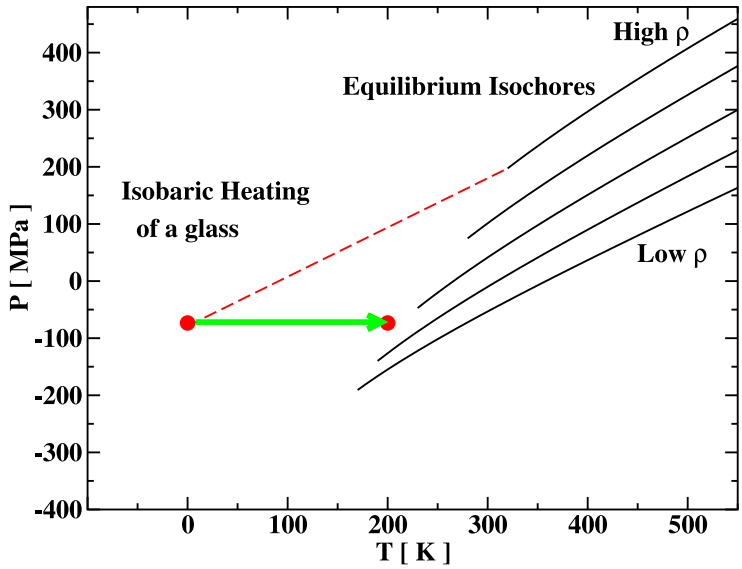

Figure 15. Representation of the numerical experimental protocol. The full black lines indicate the equilibrium equation of state for the LW-OTP model. The dashed line indicates the fast, steepest descent, constant volume quench. The green arrow indicates the heating of the glass at constant pressure, up to the liquid state.

approach and for generalizing it to out-of-equilibrium states. As long as a configuration is a typical equilibrium configuration (which properly indicates that there exists a T such that the chosen configuration is a representative equilibrium configuration), then the volume and the $e_{\rm IS}$ values are the only information required to predict other thermodynamic properties of the system (basin shape, $P_{\rm IS}$ and so on). Of course, a strong hypothesis, which lies at the basis of the validity of the OOE EOS landscape approach, is that the chosen configuration is indeed explored in equilibrium. Breakdown of such a hypothesis will be discussed in the next section.

A series of works based on the OTP potential have focused on the possibility of modelling the thermodynamics of out-of-equilibrium liquids within the landscape approach. The interested reader can refer to [71, 72]. Here I review the case of constant P heating of a glass, generated via constant V quenching of equilibrium liquid configurations. The experimental protocol (the history of the sample) is shown in figure 15. It is important to observe that the constant volume steepest descent minimization (instant quench) guarantees that the starting glass at $T = 0$ K is a frozen liquid configuration.

The OOE EOS does not provide indications of the dynamic evolution of the system, in the same way as the equilibrium thermodynamic approach does not provide information on the equilibrium dynamics. On the other hand, if information on the t dependence of the $e_{\rm IS}$ explored (which is equivalent to information on the t dependence of the effective T) is provided, then using the OOE EOS, the t dependence of the volume can be predicted and compared with the simulation results. Figure 16 shows the t dependence of the $e_{\rm IS}$, during the heating at constant pressure for the LW-OTP model. This set of $e_{\rm IS}$ data, together with the $T(t)$ and $P(t)$ values, is used to predict the t dependence of V, $P_{\rm IS}$ and any other property of the system, for example the average basin curvature. The comparisons

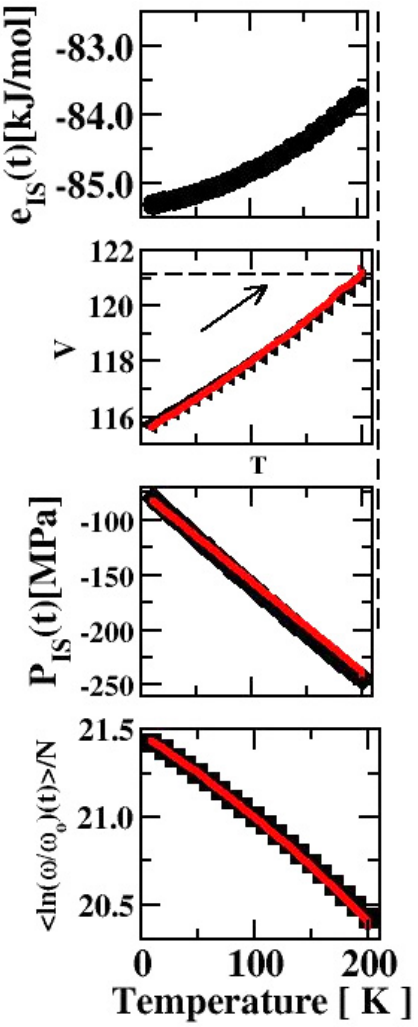

Figure 16. Evolution of thermodynamic quantities during constant pressure heating of a glass for the LW-OTP model. From top to bottom: $e_{\rm IS}$, V, $P_{\rm IS}$ and $\langle\sum_{j=1}^{6N-3}\ln(\omega_j/\omega_0)\rangle/N$. The symbols are MD data; the lines in the bottom three panels are predictions based on the landscape OOE EOS.

between the theoretical predictions and the corresponding numerical data are also shown in figure 16.

Similar agreement has been observed for constant T compression and for constant V heating. In all cases, the starting glass has been generated with steepest descent procedures and hence the starting glass structure is by construction well represented by an equilibrium liquid configuration.

12. Ageing in the PEL formalism: breakdown of the one-fictive-parameter description

The possibility of associating a glass configuration with a liquid state point via one effective temperature is the basic assumption of the landscape EOS. The results reviewed in the previous section show that when the out-of-equilibrium process does proceed via

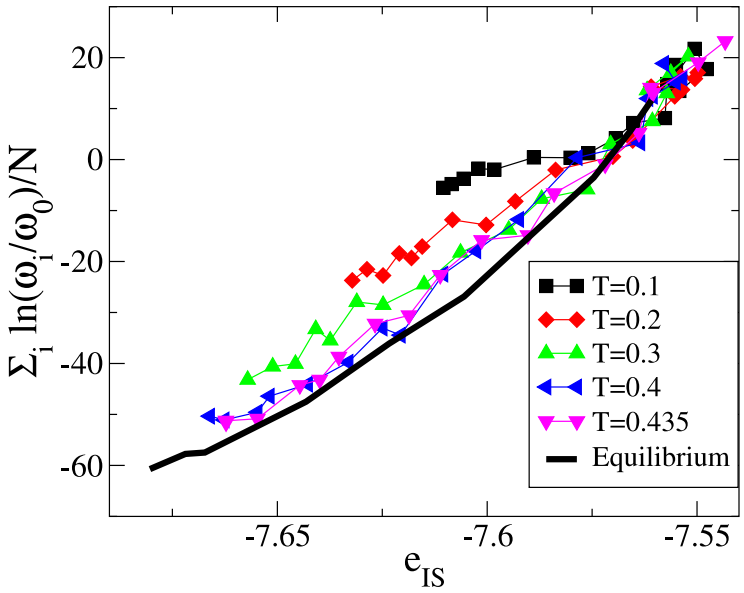

Figure 17. Basin depth dependence of the shape factor $\mathcal{S}$ calculated from equilibrium configurations at different temperatures (full line) and from ageing configurations at different times (symbols). In all cases, the ageing simulations refer to instantaneous temperature quenches from $T = 5$ to the T indicated in the label. Redrawn from [73].

states which can be connected to equilibrium configurations, the OOE thermodynamics is successful in interpreting the thermodynamic evolution of the system.

Ageing phenomena at finite T provide a case where the basic landscape assumption breaks and the OOE EOS cannot be properly used. In these cases, one additional parameter is not sufficient any longer.

Simple evidence of the breaking of the basic landscape hypothesis is provided by a comparative study of the shape of the basin explored in equilibrium and in the ageing dynamics following a T jump, at constant V for the BMLJ model. Figure 17 shows $\mathcal{S}$, defined in equation (25), calculated from IS configurations extracted from equilibrium configurations, and contrasts its $e_{\rm IS}$ dependence with the same quantity evaluated from configurations extracted in the ageing runs. At very short times, when the ageing liquid has a configuration not very different from the starting equilibrium configuration, the relation $\mathcal{S}$ versus $e_{\rm IS}$ in ageing is identical to the equilibrium one. On increasing $t_{\rm w}$, the ageing curves separate more and more from the equilibrium curve, proportionally to the bath T. For extremely deep quenches (like the $T = 0.1$ one in the figure) the decrease on the landscape takes place at almost constant $\mathcal{S}$. Only when the bath T is close to the mode coupling temperature (which for the BMLJ model has been estimated at $T \approx 0.43$ [28]) do equilibrium and ageing curves coincide.

Results shown in figure 17 suggest that only when the change of external parameters is small, or when the system is close to equilibrium, does the evolution of the equilibrating system proceed along a sequence of states which are explored in equilibrium. Under these circumstances, the location of the ageing system can be traced back to an equivalent equilibrium state, and a fictive temperature can be defined. In this approximation,

J. Stat. Mech. (2005) P05015

a thermodynamic description of the ageing system based on one additional parameter can be provided. When the external perturbation is significant, like in hyperquenching experiments [74], the ageing dynamics propagates the system along a path which is not explored in equilibrium [37, 75]. In this case it becomes impossible to associate the ageing system with a corresponding liquid configuration.

A more convincing evidence of the breakdown of the one-fictive-parameter description under ageing is provided by the so-called crossover experiment. In the previous sections, I have discussed the fact that in the case of glasses, systems in out-of-equilibrium conditions, the T and V values are not sufficient for predicting P, since the state of the system depends on its previous thermal and mechanical history. Different glasses, at the same T and V, are characterized by different P values. When it is possible to encode the previous history of the system in *only* one additional parameter, then two glasses with identical composition having not only the same T and V but also the same P are the same glass. If this is the case, the two glasses should respond to an external perturbation in the same way and should age with similar dynamics.

In the 1960s, Kovacs and co-workers designed an experimental protocol [76]–[78] for generating distinct glasses with different thermal and mechanical histories but with the same T, V and P values. Polyvinyl acetate was equilibrated at high temperature $T_{\rm h}$ and then quenched at low temperature $T_{\rm l}$, where it was allowed to relax isothermally for a waiting time $t_{\rm w}$ insufficient for reaching equilibrium. The material was then reheated to an intermediate temperature T, and allowed to relax. The entire experiment was performed at constant pressure P. The observed dynamics of the volume relaxation toward equilibrium—in the last step at constant T and P—was striking; the volume crosses over the equilibrium value, passes through a maximum, which depends upon the actual thermal history of the system, and then relaxes to the equilibrium value. The existence of a maximum clearly indicates that there are states with the same V (to the left and to the right of the maximum) which, although T, V and P are the same, evolve differently. Thus, this experiment strongly supports the idea that one additional effective variable is not sufficient for uniquely predicting the state of the glass.

Recently, the Kovacs experiment (also known as the crossover experiment) has been reproduced numerically (see figure 18), to develop intuition as regards the differences between states with the same T, V and P and the conditions under which out-of-equilibrium thermodynamics may be used to describe glass states. It has been found that for sufficiently deep quenching temperatures, and long ageing times, following the protocol proposed by Kovacs, it is indeed possible to identify two distinct states with the same T, V and P which evolve in different ways. When the system is forced to age following large amplitude T jumps, i.e., at low $T_{\rm l}$, it starts to explore regions of the landscape which are never explored in equilibrium. Under these conditions, it is not possible any longer to associate a glass with a 'frozen' liquid configuration via the introduction of a fictive temperature or pressure.

It is a challenge for future studies to find whether a thermodynamic description can be recovered by decomposing the ageing system into a collection of substates, each of them associated with a different fictive temperature—a picture somehow encoded in the phenomenological approaches of Tool and co-workers [79] and Kovacs and co-workers [80]—or whether the glass, produced under extreme perturbations, freezes in some highly stressed configuration which can never be associated with a liquid state. Studies of

J. Stat. Mech. (2005) P05015

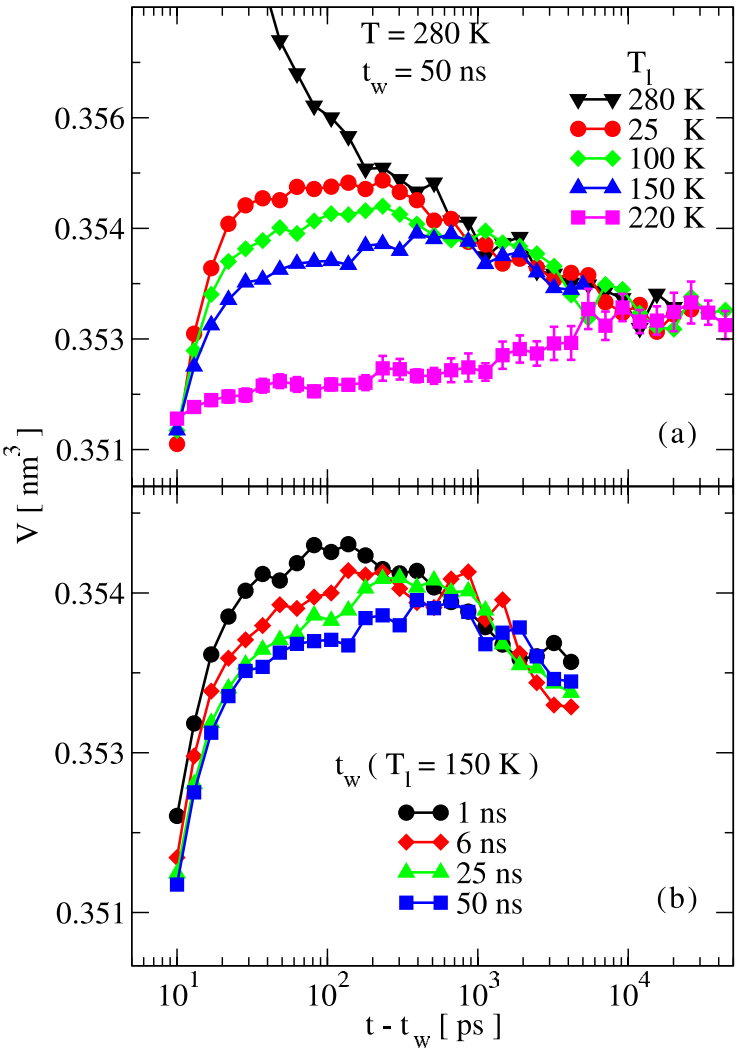

Figure 18. Volume relaxation showing the crossover effect in a molecular system. Top: a system of 343 OTP molecules at constant $P = 16$ MPa is equilibriated at $T_\mathrm{h} = 400$ K, quenched at several low temperatures T_l and left to age for $t_e = 50$ ns, a time insufficient for reaching equilibrium at T_l. The system is then heated at the intermediate temperature $T = 280$ K and the V relaxation dynamics is recorded (symbols). For the case $T_\mathrm{l} = T$, the system is directly brought from $T_\mathrm{h} = 400$ to $T = 280$ K and hence $t_\mathrm{w} = 0$. For time shorter than 20 ps, T and P have not yet equilibrated to the final values. Bottom: volume relaxation at $T = 280$ K, at fixed $T_\mathrm{l} = 150$ K for different t_w values.

the fluctuations around the mean values [52] will help in understanding differences between the landscapes explored by the system in equilibrium and in ageing; the hope is that some of you will be able to formulate a thermodynamic approach of wider applicability.

Acknowledgments

These notes cover a significant fraction of my own research in the last 10 years. I am grateful to all colleagues with whom I had the pleasure of collaborating and interacting.

In particular, I would like to mention, in random order, P Tartaglia, P Poole, S Sastry, P Debenedetti, R Speedy, E La Nave, S Mossa, A Scala, I Saika-Voivod, C De Michele, A Moreno, A Angell, S Franz, D Wales, N Giovambattista, H E Stanley, F Starr and W Kob.

References

[1] Götze W, 1999 *J. Phys.: Condens. Matter* **11** A1
[2] Debenedetti P G, 1997 *Metastable Liquids* (Princeton, NJ: Princeton University Press)
[3] Debenedetti P G and Stillinger F H, 2001 *Nature* **410** 259
[4] Angell C A, 1995 *Science* **267** 1924
[5] Angell C A, 1991 *J. Non-Cryst. Solids* **131** 13–31
[6] Kauzmann A W, 1948 *Chem. Rev.* **43** 219
[7] Martinez L M and Angell C A, 2001 *Nature* **410** 663
[8] Goldstein M, 1969 *J. Chem. Phys.* **51** 3728
[9] Ruocco G *et al*, 2004 *J. Chem. Phys.* **120** 10666 and references therein
[10] Keyes T, 1997 *J. Phys. Chem.* **101** 2921
Li W-X and Keyes T, 1999 *J. Chem. Phys.* **111** 5503
Keyes T, 1994 *J. Chem. Phys.* **101** 5081
Gezelter J D *et al*, 1997 *J. Chem. Phys.* **107** 4618
Bembenek S D and Laird B B, 2001 *J. Chem. Phys.* **114** 2340
Donati C, Sciortino F and Tartaglia P, 2000 *Phys. Rev. Lett.* **85** 1464
La Nave E, Scala A, Starr F W, Sciortino F and Stanley H E, 2000 *Phys. Rev. Lett.* **84** 4605
La Nave E, Scala A, Starr F W, Sciortino F and Stanley H E, 2001 *Phys. Rev.* E **64** 036102
Angelani L, Di Leonardo R, Ruocco G, Scala A and Sciortino F, 2000 *Phys. Rev. Lett.* **85** 5356
Broderix K, Bhattacharya K K, Cavagna A, Zippelius A and Giardina I, 2000 *Phys. Rev. Lett.* **85** 5360
Cavagna A, 2001 *Europhys. Lett.* **53** 490
Angelani L, Di Leonardo R, Ruocco G, Scala A, Sciortino F and Cavagna A, 2002 *J. Chem. Phys.* **116** 10297
Angelani L, Ruocco G, Sampoli M and Sciortino F, 2003 *J. Chem. Phys.* **118** 5265
Hurley M and Harrowell P, 1995 *Phys. Rev.* E **52** 1694
Fynewever H, Perera D and Harrowell P, 2000 *J. Phys.: Condens. Matter* **12** A399
[11] Wales D J, 2004 *Energy Landscapes* (Cambridge: Cambridge University Press)
[12] Stillinger F H and Weber T A, 1982 *Phys. Rev.* A **25** 978
Stillinger F H and Weber T A, 1984 *Science* **225** 983
Stillinger F H, 1995 *Science* **267** 1935
[13] Wales D J, 2001 *Science* **293** 2067
[14] Kopsias N P and Theodorou D N, 1998 *J. Chem. Phys.* **109** 8573
[15] Middleton T F and Wales D J, 2003 *J. Chem. Phys.* **118** 4583
[16] Stillinger F H, 1998 *J. Phys. Chem.* B **102** 2807
[17] Richert R and Angell C A, 1998 *J. Chem. Phys.* **108** 9016
[18] Speedy R J, 2001 *J. Phys. Chem.* B **105** 11737
[19] La Nave E, Mossa S, Sciortino F and Tartaglia P, 2004 *J. Chem. Phys.* **120** 13
[20] Sastry S, Debenedetti P G and Stillinger F H, 1977 *Phys. Rev.* E **56** 5533
[21] Frenkel D and Smit B, 1996 *Understanding Molecular Simulation* (San Diego, CA: Academic)
[22] Coluzzi B, Parisi G and Verrocchio P, 2000 *Phys. Rev. Lett.* **84** 306
[23] Sciortino F, Kob W and Tartaglia P, 1999 *Phys. Rev. Lett.* **83** 3214
[24] La Nave E, Mossa S, De Michele C, Sciortino F and Tartaglia P, 2003 *J. Phys.: Condens. Matter* **15** S1085
[25] Mossa S, La Nave E, Stanley H E, Donati C, Sciortino F and Tartaglia P, 2002 *Phys. Rev.* E **65** 041205
[26] Press W H, Flannery B P, Teukolsky A A and Vetterling W T, 1986 *Numerical Recipes: The Art of Scientific Computing* (Cambridge: Cambridge University)
[27] Stillinger F H and Weber T A, 1985 *Phys. Rev.* B **31** 5262
[28] Kob W and Andersen H C, 1995 *Phys. Rev.* E **51** 4626
Kob W and Andersen H C, 1995 *Phys. Rev.* E **52** 4134
[29] van Beest B W H, Kramer G J and van Santen R A, 1990 *Phys. Rev. Lett.* **64** 1955
[30] Lewis L J and Wahnström G, 1994 *Phys. Rev.* E **50** 3865

[31] Berendsen H J C, Postma J P M, Van Gunsteren W F, Dinola A and Haak J R, 1984 *J. Chem. Phys.* **81** 3684
[32] Stillinger F H and Weber T A, 1983 *Phys. Rev.* A **28** 2408
[33] Heuer A, 1997 *Phys. Rev. Lett.* **78** 4051
[34] Sastry S, Debenedetti P G and Stillinger F H, 1998 *Nature* **393** 554
See also the related work of Jonsson H and Andersen H C, 1988 *Phys. Rev. Lett.* **60** 2295
[35] Scheidler P, Kob W, Latz A, Horbach J and Binder K, 2001 *Phys. Rev.* B **63** 104204
[36] Starr F W, Sastry S, La Nave E, Scala A, Stanley H E and Sciortino F, 2001 *Phys. Rev.* E **63** 041201
[37] Giovambattista N, Stanley H E and Sciortino F, 2003 *Phys. Rev. Lett.* **91** 115504
[38] Sciortino F, La Nave E and Tartaglia P, 2003 *Phys. Rev. Lett.* **91** 155701
[39] Sastry S, 2001 *Nature* **409** 164
[40] Keyes T and Chowdhary J, 2004 *Phys. Rev.* E **69** 041104
[41] Moreno A *et al*, 2004 *Preprint* cond-mat/0407801
[42] Frenkel D and Ladd A J C, 1984 *J. Chem. Phys.* **81** 3188
[43] Coluzzi B, Mezard M, Parisi G and Verrocchio P, 1999 *J. Chem. Phys.* **111** 9039
[44] Angelani L, Foffi G, Sciortino F and Tartaglia P, 2005 *J. Phys.: Condens. Matter* **17** L113
[45] Deridda B, 1981 *Phys. Rev.* B **24** 2613
[46] Keyes T, 2000 *Phys. Rev.* E **62** 7905
[47] Heuer A and Buchner S, 2000 *J. Phys.: Condens. Matter* **12** 6535
[48] La Nave E, Mossa S and Sciortino F, 2002 *Phys. Rev. Lett.* **88** 225701
[49] Middleton T F, Hernandez-Rojas J, Mortenson P N and Wales D J, 2001 *Phys. Rev.* B **64** 184201
[50] Fernandez J R and Harrowell P, 2004 *J. Chem. Phys.* **120** 9222
Fernandez J R and Harrowell P, 2003 *Phys. Rev.* E **67** 011403
[51] La Nave E and Sciortino F, 2004 *J. Phys. Chem.* B **108** 19663
[52] Saika-Voivod I and Sciortino F, 2004 *Phys. Rev.* E **70** 041202
[53] Sciortino F, Kob W and Tartaglia P, 2000 *J. Phys.: Condens. Matter* **12** 6525
[54] Büchner S and Heuer A, 1999 *Phys. Rev.* E **60** 6507
[55] Scott Shell M, Debenedetti P G, La Nave E and Sciortino F, 2003 *J. Chem. Phys.* **118** 8821
[56] La Nave E, Sciortino F, Tartaglia P, Shell M S and Debenedetti P G, 2003 *Phys. Rev.* E **68** 032103
[57] Speedy R J, 2003 *J. Phys.: Condens. Matter* **15** S1243
[58] De Michele C, Sciortino F and Coniglio A, 2004 *J. Phys.: Condens. Matter* **16** L489
[59] Hansen J P and McDonald I R, 1986 *Theory of Simple Liquids* 2nd edn (New York: Academic)
[60] Jund P and Jullien R, 1999 *Phys. Rev. Lett.* **83** 2210
[61] Bembenek S D and Laird B B, 2001 *J. Chem. Phys.* **114** 2340
[62] Saika-Voivod I, Poole P H and Sciortino F, 2001 *Nature* **412** 514
[63] La Nave E, Stanley H E and Sciortino F, 2002 *Phys. Rev. Lett.* **88** 035501
[64] Saika-Voivod I, Poole P H and Sciortino F, 2004 *Phys. Rev.* E **69** 041503
[65] Saksaengwijit A, Reinisch J and Heuer A, 2004 *Phys. Rev. Lett.* **93** 235701
[66] Horbach J and Kob W, 1999 *Phys. Rev.* B **60** 3169
[67] Bouchaud J-P, Cugliandolo L F, Kurchan J and Mézard M, 1998 *Spin Glasses and Random Fields* ed A P Young (Singapore: World Scientific) pp 161–223
[68] Cugliandolo L F, Kurchan J and Peliti L, 1997 *Phys. Rev.* E **55** 3898
[69] Franz S and Virasoro M A, 2000 *J. Phys. A: Math. Gen.* **33** 891
[70] La Nave E, Sciortino F, Shell M S and Debenedetti P G, 2005 *Phys. Rev.* E **71** 033102
[71] Mossa S, La Nave E, Sciortino F and Tartaglia P, 2002 *Eur. Phys. J.* B **30** 351
[72] Mossa S, La Nave E, Tartaglia P and Sciortino F, 2003 *J. Phys.: Condens. Matter* **15** S351
[73] Mossa S, Ruocco G, Sciortino F and Tartaglia P, 2002 *Phil. Mag.* B **82** 695–705
[74] Velikov V, Borick S and Angell C A, 2002 *J. Phys. Chem.* B **106** 1069
Angell C A, Yue Y, Wang L-M, Copley J R D, Borick S and Mossa S, 2003 *J. Phys.: Condens. Matter* **15** S1051
[75] Mossa S and Sciortino F, 2004 *Phys. Rev. Lett.* **92** 045504
[76] Kovacs A J, 1963 *Fortschr. Hochpolym. Forsch.* **3** 394
[77] McKenna G B, 1989 *Comprehensive Polymer Science* (*Polymer Properties* vol 2) ed C Booth and C Price (Oxford: Pergamon) pp 311–62
[78] Angell C A, Ngai H L, McKenna G B, McMillan P F and Martin S W, 2000 *J. Appl. Phys.* **88** 3113
[79] Tool A Q, 1946 *J. Am. Ceram. Soc.* **29** 240
[80] Kovacs A, Aklonis J J, Hutchinson J M and Ramos A R, 1979 *J. Polym. Sci., Polym. Phys. Edn Engl.* **17** 1097

J. Stat. Mech. (2005) P05015